INSTITUTE OF
PAPER CHEMISTRY
Appleton · Wisconsin

FUME GENERATION FROM ALKALI
CARBONATE / SULFIDE MELTS

Project 3473-1

Report Four
A Progress Report
to
MEMBERS OF THE INSTITUTE OF PAPER CHEMISTRY

May 15, 1986

NOTICE & DISCLAIMER

THE INSTITUTE OF PAPER CHEMISTRY

Appleton, Wisconsin

FUME GENERATION FROM ALKALI CARBONATE/SULFIDE MELTS

Project 3473-1

Report Four

A Progress Report

to

MEMBERS OF THE INSTITUTE OF PAPER CHEMISTRY

May 15, 1986

TABLE OF CONTENTS

LIST OF TABLES

LIST OF FIGURES

THE INSTITUTE OF PAPER CHEMISTRY

Appleton, Wisconsin

FUME GENERATION FROM ALKALI CARBONATE/SULFIDE MELTS

EXECUTIVE SUMMARY

This is one report in a series describing the fundamental processes occurring in the kraft recovery furnace. This report is concerned with the processes responsible for fume generation.

Fume in the kraft recovery furnace has both detrimental and beneficial effects. High fume generation rates contribute to the precipitator dust collection loads, increase the soot blowing requirements, and contribute to fouling of heat transfer surfaces and plugging of gas passages. The beneficial aspect of fume is that it acts as a scavenger for SO_2. The fume compounds react with SO_2 to form Na_2SO_4, which is removed by the precipitators and recycled back into the black liquor. Low fume generation rates may result in high levels of SO_2 and associated sticky deposits.

A major portion of this report is devoted to understanding the processes responsible for fume generation during Na_2S oxidation. Air oxidation of Na_2S in Na_2S/Na_2CO_3 melts was found to produce copious quantities of Na_2CO_3 fume. The fume generation rate was over an order of magnitude greater than that observed under reducing conditions. This phenomenon was unexpected and very difficult to interpret in terms of existing concepts of fume by formation and volatilization of elemental Na or through the formation and volatilization of NaOH.

At first, fuming during sulfide oxidation was thought to be an entirely new and likely dominant fuming process. This research has shown that it is a manifestation of enhanced mass transfer resulting from gas phase oxidation of the

volatile species. This gas-phase oxidation reaction is a dominant feature of fume generation in an oxidizing environment.

Based on the experimental results obtained in this study, the large quantity of fume which can be generated during sulfide oxidation was determined to be a result of Na oxidation in the gas phase. Oxidation of Na in the gas phase significantly lowers the partial pressure of Na. Since the driving force for vaporization is the difference between the equilibrium vapor pressure of Na at the gas-melt interface and the partial pressure of Na in the gas phase, this reduction in partial pressure of Na significantly increases Na vaporization.

One of the main experimental results supporting this conclusion is the effect of the mode of gas-melt contact on the amount of fume produced. Oxidation of a Na_2S/Na_2CO_3 melt with the N_2/O_2 purge introduced below the melt's surface produced copious quantities of Na_2CO_3 fume. Fume generation was only slightly dependent on the O_2 content of the purge, almost directly proportional to the N_2 purge rate, and had an Arrhenius type temperature dependence with an activation energy of approximately 20,000 cal/mole. On the other hand, oxidation of a Na_2S/Na_2CO_3 melt with the N_2/O_2 purge introduced above the melt's surface produced relatively little fume. In this mode of gas-melt contact, fume generation decreased with an increase in the O_2 content of the purge.

This dramatic difference in fuming behavior observed between the two modes of gas-melt contact results from the Na_2S oxidation reaction being mass transfer limited in the liquid phase when the purge is introduced above the melt and mass transfer limited in the gas phase when the purge is introduced below the melt's surface. With the purge introduced above the melt's surface, the liquid

at the interface consists principally of Na_2CO_3 and Na_2SO_4. Since the vapor

pressure of Na is very low in this Na_2CO_3/Na_2SO_4 layer, little Na is vaporized.

With the purge introduced below the melt's surface, the melt at the

interface is renewed faster than oxygen can be supplied to the melt. This

results in Na_2S oxidation being gas side limited and the level of Na at the

interface being relatively high. This situation is illustrated in Fig. 1. The

relatively high Na vapor pressure results from the equilibrium reaction of

Na_2CO_3 with Na_2S. The Na then vaporizes and reacts with CO_2 and O_2 to form Na_2CO_3.

This gas phase reaction lowers the partial pressure of Na in the gas phase and

significantly increases the Na fuming rate.

$$O_2 \text{ flux}$$

$$\text{Gas} \quad \text{Phase}$$
$$\tfrac{1}{2}O_2 + CO_2 + 2Na \longrightarrow Na_2CO_3 \; (\text{fume})$$

$$\delta \quad Na, CO_2 \text{ flux}$$

Gas—Melt
Interface

$$\text{Liquid Phase}$$

$$Na_2CO_3 + \tfrac{1}{4}Na_2S \rightleftharpoons \tfrac{1}{4}Na_2SO_4 + CO_2 + 2Na$$
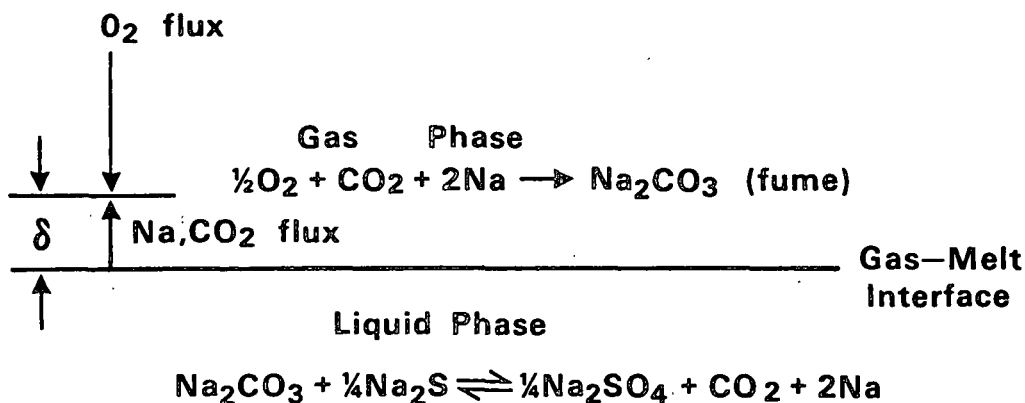
Figure 1. Fume generation under oxidizing conditions.

Other fume generation processes discussed in this report include fume

generation under reducing conditions, the effect of NaOH on fume generation, and

the behavior of K and Cl during fume generation. Fume in the kraft recovery

furnace has been attributed to the volatilization of Na resulting from the high

temperature and reducing conditions present in the furnace bed. Fume generation

under reducing conditions was studied using partial H_2 and CO_2 atmospheres and

by adding kraft char to the melt. Considerably less fume was produced under these conditions than was produced during sulfide oxidation.

The effect of NaOH was studied by adding NaOH pellets to the melt. Relative to fume generation during sulfide oxidation, the addition of the NaOH pellets produced little fume.

Another area of interest in fume generation is the behavior of K and Cl. Fume in the kraft recovery furnace is enriched in these elements, which lower the melting point of the deposits on the heat transfer surfaces and which may also form corrosive environments within these deposits. The behavior of these elements during fume generation was studied by adding K and Cl compounds to Na_2CO_3/Na_2S melts, monitoring the fume generation rate under various experimental conditions, and analyzing the fume.

Chloride enrichment was found to result from the vaporization of NaCl and KCl. Potassium enrichment was found to result from KCl being more volatile than NaCl.

The major conclusions reached in this study are summarized below:

1. Fume production is a dynamic process, dependent on mass transfer processes and chemical reactions. This implies that fume in a kraft recovery furnace is more than an equilibrium phenomenon and that it may be possible to manipulate the fume generating process.

2. Sodium vaporization can be significant during sulfide oxidation in a $Na_2CO_3-Na_2S$ melt and can result in large quantities of Na_2CO_3 fume. This was an unexpected result, since Na is a reduced species and was previously not thought to be present during an oxidative process.

3. Fume produced during sulfide oxidation results from the oxidation of Na vapor in the gas phase. This oxidation of Na produces a Na sink in the gas phase, reducing the partial pressure of Na and the mass transfer resistance to vaporization. This vapor sink significantly increases the rate of Na vaporization.

4. Only when the purge was introduced below the melt's surface did sulfide oxidation produce sufficient quantities of fume. The oxidation of sulfide in a quiescent melt with the N_2-O_2 purge introduced above the melt's surface produced little fume. In this situation, the volatile species were oxidized before they could evolve from the melt. With the N_2-O_2 purge introduced below the melt's surface, the melt at the interface was renewed faster than it was oxidized. Volatile species were then present at the interface and produced large quantities of fume.

5. Fume generation resulting from reduction of Na_2CO_3 with carbon, H_2 or CO is significantly lower than fume generation during sulfide oxidation in a well mixed melt. The addition of CO to the purge in a Na_2CO_3/Na_2S melt did not result in an increased level of fume generation over that observed with a N_2 purge. The addition of carbon in the form of kraft or soda char and the addition of H_2 to a Na_2CO_3/Na_2S melt only slightly increased the level of fume generation over that observed under a N_2 purge.

6. The addition of NaOH pellets to a Na_2CO_3/Na_2S melt did not result in any increase in fume generation. Sodium hydroxide levels as great as 4.5% did not result in significant fume.

No evidence was obtained that the presence of NaOH in the melt contributes to fume.

7. Sodium and potassium chloride are more volatile than Na_2CO_3 and K_2CO_3. This results in the fume being enriched in Cl. Since KCl is more volatile than NaCl, the fume is also enriched in K. Equilibrium considerations may govern the volatilization of NaCl and KCl.

8. The only volatile species that contribute to the formation of fume in the kraft furnace are Na vapor, K vapor, NaCl vapor and KCl vapor.

   a) No evidence was found for NaOH volatilizing as such from a carbonate melt and forming NaOH vapor.

   b) No evidence was found to support a role played by volatile alkali metal oxides.

INTRODUCTION

This report describes an experimental study of fume generation from alkali carbonate/sulfide melts. Sodium carbonate and sodium sulfide are the principal inorganic compounds present in the kraft recovery furnace. Fume is submicron inorganic particles formed from the vaporization of the inorganic salts and condensation of these salts in the gas phase. The principal objective of this study was to identify the processes responsible for fume generation and to determine the effect of the experimental variables on these processes.

Fume generation within the kraft recovery furnace has usually been considered to be due to Na volatilization resulting from the high temperature and reducing conditions present in the char bed. Equilibrium diagrams predict that sodium volatilization becomes significant at temperatures above 930°C (1700°F) and increases with temperature and the strength of the reducing environment. Borg[1] applied equilibrium considerations to a Gotaverken (B&W) type furnace. He concluded that the fume generation rate is controlled by the furnace zones with the highest average temperature. These zones are the secondary air/liquor spray level and the bed surface. At 1930°F, the fume production rate predicted by equilibrium considerations corresponded closely to that observed in the furnace. Warnqvist[2] also used chemical equilibrium calculations to predict the effect of furnace variables on sodium and sulfur emissions. In addition to sodium (Na and Na_2), Warnqvist also predicted that the formation and volatilization of NaOH is a primary source of fume. These treatments of fume generation as an equilibrium process suggest that there is little that can be done to control fuming other than manipulating furnace temperatures.

Fume generation significantly affects the design and operation of a kraft recovery furnace. One of the major effects of fume is the formation of

substantial deposits on the heat transfer surfaces. This results in the need

for greater heat transfer area for a given steam load and the use of soot-blow-

ing steam to remove these deposits. Typically 3 to 7% of the steam generated is

used for soot-blowing.[3] When deposits are severe, they may result in plugging

of gas passages and require periodic boiler shutdown for their removal. The

fume particles that do not form deposits are collected by the precipitator and

recycled into the strong black liquor.

A major finding described in this report is the mechanism for fume

generation under oxidizing conditions. Air oxidation of sulfide was found to

produce over an order of magnitude more fume than strongly reducing conditions.

This was an unexpected result not predicted by equilibrium calculations. When

first observed this phenomenon appeared to be a new and dominant fuming process

under conditions similar to those in the kraft furnace. The primary focus of

this research was then to understand fuming under oxidizing conditions.

PROJECT OBJECTIVES

The primary objective of this study was to understand the processes re-

sponsible for fume production during sulfide oxidation. To achieve this objective,

kinetic data were obtained on oxidative fuming. The fundamental kinetic data

include experimental data on the effects of the melt composition, temperature,

oxidizing and reducing environment, and mode of gas-liquid contact. Other objec-

tives were to measure fume under various reducing conditions, study the effect

of NaOH on fume, and define the process responsible for K and Cl fume enrichment.

The two principal processes occurring within the kraft recovery furnace

are the burning of the organic content of the kraft black liquor and the reduc-

tion of the sulfur species present to Na_2S. The burning of carbon content of

kraft char has been shown to occur through a sulfate-sulfide cycle. In this cycle, the Na_2SO_4 present in the char is reduced by the carbon to Na_2S and the carbon is oxidized to CO_2 and CO. The Na_2S is then reoxidized by O_2 completing the cycle. The burning of carbon through this cycle is illustrated in Fig. 2.
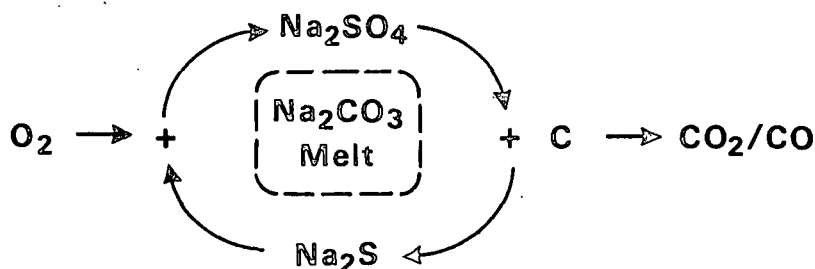
Figure 2. Sulfate-sulfide cycle.

Since the burning of the carbon content of the kraft black liquor char occurs through this sulfate-sulfide cycle, sulfide oxidation is continually occurring in the kraft furnace. Sulfide oxidation also occurs anytime oxygen comes into contact with reduced smelt. Therefore, considerable sulfide oxidation occurs in the kraft recovery furnace and may be responsible for a major portion of the fume generated in the furnace.

The major experimental objectives are to

1. Determine if fuming is inherent during sulfide oxidation, hence char burning, or if it depends on special experimental conditions. If fume production is an inherent part of char burning, it is unlikely that changes in the furnace operation would have a large effect on fume generation. If, however, fume production depends on the experimental conditions, it would be manipulable, depending on how black liquor is burnt.

2. Design an experimental system to acquire data on fume generation over a wide range of experimental conditions.

BACKGROUND

FUME GENERATION IN RECOVERY FURNACES

Fume in a kraft recovery furnace originates from the vaporization and condensation of inorganic salts. It consists of very fine dustlike particles typically 0.25 to 1.0 μm in diameter. Fume has usually been attributed to Na vaporization resulting from the high temperatures and reducing conditions present in the furnace. Some of the reducing reactions that can occur in the furnace are shown below.

$$Na_2CO_3 + 2C \rightleftharpoons 2Na + 3CO \tag{1}$$

$$Na_2CO_3 + CO \rightleftharpoons 2Na + 2CO_2 \tag{2}$$

$$Na_2CO_3 + H_2 \rightleftharpoons 2Na + CO_2 + H_2O \tag{3}$$
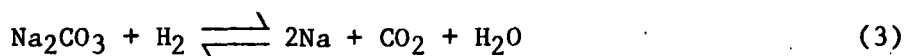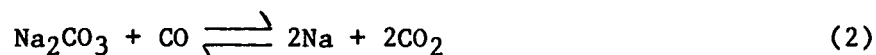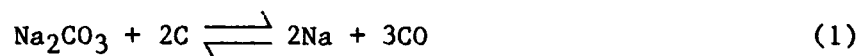
The Na produced through these reactions can react with the furnace gases to produce Na_2SO_4 and Na_2CO_3, as given by Eq. (4)-(7). These condense into fume particles.

$$2Na + 1/2O_2 \rightleftharpoons Na_2O \tag{4}$$

$$Na_2O + CO_2 \rightleftharpoons Na_2CO_3 \tag{5}$$

$$Na_2CO_3 + SO_2 + 1/2O_2 \rightleftharpoons Na_2SO_4 + CO_2 \tag{6}$$

$$Na_2O + SO_2 + 1/2O_2 \rightleftharpoons Na_2SO_4 \tag{7a}$$

$$Na_2O + SO_3 \rightleftharpoons Na_2SO_4 \tag{7b}$$
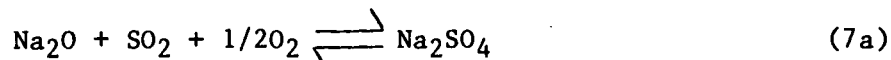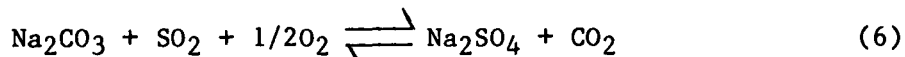
Another possible source of fume is the formation of NaOH, a relatively volatile compound which can be formed through the reaction of H_2O with Na_2CO_3, Eq. (8).

$$Na_2CO_3 + H_2O \rightleftharpoons CO_2 + 2NaOH \qquad\qquad (8)$$
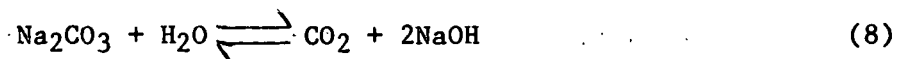
These fume particles can deposit on the heat transfer surfaces in the boiler, reducing the heat transfer coefficient and creating conditions favorable for corrosion. These deposits may eventually plug gas passages in the boiler and economizer and require unscheduled shutdowns for their removal.

From the examination of deposits formed on air cooled probes, Reeve et al.[4] concluded that deposits are formed by two different mechanisms. In the first mechanism, black liquor droplets are entrained in the furnace gases and burn, leaving a residue of the inorganic salts. These burnt black liquor particles then strike and adhere to the heat transfer surfaces. In the second mechanism, inorganic compounds vaporize in the lower furnace and condense on the cooler heat transfer surfaces forming deposits. Reeve et al.[4] found that the deposits in the lower superheater, especially in the front side of the tubes, resulted primarily from carry-over. In the upper superheater and boiler bank condensation of the fume on the tubes was more important in deposit formation.

Borg et al.[1] conducted a study of the origins of the S and Na emissions in a Götaverken (B&W type) boiler. From electron microscopy studies, two types of particles were identified: those formed by entrainment and burning of black liquor droplets and those formed from vaporization of inorganic compounds in the lower furnace and condensation of these compounds in furnace gases. From the particle sizes it is found that the weight percentage of actual carry-over (burnt liquor particles) was very small (less than 1 wt.%) compared to the fume particles. However, the location at which the particles were collected was not identified, and it is well known that carry-over particles, being heavier, tend to drop out of the gas stream before the precipitators.

Rizhinshvili et al.[5] conducted a study on the emissions from a recovery furnace and also reported the two types of particles. The large burnt liquor particles had a diameter of 2 to 20 mm, while the smaller fume particles were submicron. The coarse fraction was present in large quantities at the black liquor spray and tertiary air levels. Being relatively large particles, they settled out in the boiler and economizer hoppers and were practically absent from the gas stream after the economizer. The percentage of carry-over in the boiler hoppers was dependent on the level of excess air and ranged from 1 to 8 wt.% of the load in the hoppers. Not more than 3% of the total emissions from the furnace was collected in the boiler and economizer hoppers. Analysis of the fume particles revealed that they were composed principally of Na_2CO_3 and Na_2SO_4 and did not contain any organic compounds, free carbon or NaOH.

The results of the studies by Borg et al.[1] and Rizhinshvili[5] indicate that a major source of particles in recovery furnaces is the vaporization of inorganic salts in the lower furnace, followed by reaction with the furnace gases and condensation. Although the majority of the particles in these studies consisted of true fume (particles formed through evaporation and condensation), carry-over also has a significant effect on boiler operation. One of the reasons for the low level of carry-over is that the carry-over tends to settle out of the gas stream in the regions of the superheater and boiler bank. The level of carry-over also depends on furnace operation (black liquor droplet size and excess air level) and may be considerably higher in some furnaces than the levels reported in these studies. Carry-over is believed to be the major cause of boiler pluggage.

FUMING IN OTHER SYSTEMS

There are two mechanisms for enhanced vaporization of a liquid into a reactive gas: (1) the gas may react with the liquid to form a volatile species or (2) the gas may react with the vapor from the liquid, lowering the partial pressure of the vapor above the liquid and enhancing the vaporization rate.

During the oxidation of many molten metals large amounts of metal oxide fumes are generated.[6-8] Since there are several similarities between these fuming systems and fuming during sulfide oxidation in a carbonate melt, a review of fuming during oxidation of molten metals is included here.

Metals in which fume generation during oxidation has been studied include Cu, Co, Mn, Ni, Fe, and Cr.[6] During oxidation of these molten metals, the rate of vaporization increases several orders of magnitude.

Another system in which an increase in fuming rate results from oxidation is the decarbonization of iron.[8] As the carbon content of the melt is oxidized, a large quantity of iron oxide fume is generated.

The increase in fuming during oxidation is attributed to the reaction of the metal vapor with oxygen to form a condensed metal oxide fume. This may be considered to be a counterflux transport process. Oxygen diffuses toward the molten metal surface, and metal vapor diffuses away from the surface. At some distance from the surface the metal vapor and oxygen react to form a metal oxide condensed phase (Fig. 3).

The rate of the metal vaporization is dependent on the rate of diffusion of the metal vapor away from the metal surface. For a molten metal with inert gas-oxygen mixture blowing across the surface, the rate of diffusion of the metal vapor is described by Eq. (9).

$$J_m = \frac{D_m}{\delta\, RT}\, (p_m{}^* - p_m)\ \text{moles/cm}^2\text{-s} \tag{9}$$

Here, J_m is the molar flux of the metal vapor;

D_m is the diffusivity of the metal vapor;

δ is the distance from the metal surface where the metal oxide is being formed;

R is the gas constant;

T is the absolute temperature;

$p_m{}^*$ is the vapor pressure of the metal at the surface; and

p_m is the partial pressure at δ where the metal oxide is being formed.

Since $p_m \ll p_m{}^*$, Eq. (9) can be rewritten as:

$$J_m = \frac{D_m}{\delta\, RT}\, p_m{}^* \tag{10}$$

Oxidation Enhanced Metal Vaporization
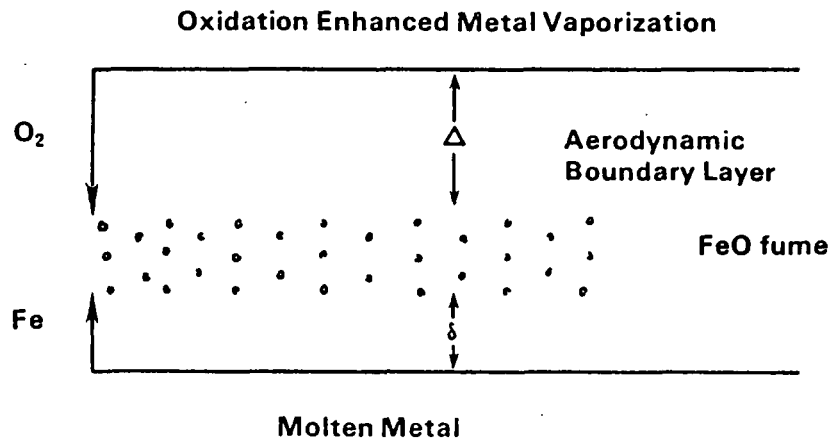
Figure 3. Gas phase oxidation enhanced vaporization.

A similar expression can be written for the flux of oxygen toward the metal surface. Oxygen diffuses from a distance above the melt, Δ, where the oxygen partial pressure is constant through an aerodynamic boundary layer to the area of the oxygen-metal vapor reaction, distance δ from the melt. The molar flux of oxygen toward the metal surface is then described by Eq. (11).

$$J_{O_2} = \frac{-D_{O_2}}{(\Delta - \delta)RT} (P_{O_2} - P'_{O_2}), \text{ moles/cm}^2\text{-s} \tag{11}$$

Here J_{O_2} is the molar flux of oxygen;

   D_{O_2} is the diffusivity of oxygen;

   P_{O_2} is the partial pressure of oxygen at distance Δ; and

   P'_{O_2} is the partial pressure of oxygen at distance δ from the partial melt surface

   Since $P_{O_2} \gg P'_{O_2}$, and $\Delta \gg \delta$, Eq. (11) can be written as:

$$J_{O_2} = \frac{-D_{O_2} \ P_{O_2}}{\Delta \ RT} \tag{12}$$

At distance δ, the metal vapor is reacting with oxygen to form the metal oxide. If one mole of metal reacts with one mole of oxygen, then $J_m = -J_{O_2}$. The flux of metal vapor from the metal surface is then described by Eq. (13).

$$J_m = \frac{D_{O_2} \ P_{O_2}}{\Delta \ RT} \tag{13}$$

For an inert gas-oxygen mixture blowing across the melt, Eq. (13) predicts that the vaporization of metal should be directly proportional to the oxygen partial pressure in the bulk gas.

The maximum rate of the metal vaporization with this mechanism is the equivalent to the rate of vaporization in a vacuum. At the maximum vaporization rate, the metal oxide fume is forming at the metal surface. If the oxygen partial pressure is increased beyond this value, the flux of oxygen toward the metal surface is greater than the vaporization rate of the metal. Oxidation then occurs within the molten metal, forming a metal oxide film. This metal oxide film results in a significant decrease in the vaporization rate of the metal.

The dependence of fume generation on oxygen partial pressure for a typical molten metal is illustrated in Fig. 4. An inert gas-oxygen mixture is passed over the melt and the rate of metal oxide fume generation is measured. As illustrated in this figure, the fume generation rate is initially proportional to the oxygen partial pressure in the gas phase. However, as the oxygen partial pressure is further increased, the fume generation rate abruptly falls to zero at a certain oxygen partial pressure. This sudden decrease in fuming results from oxidation of the metal within the melt forming a layer of metal oxide at the metal surface. This metal oxide film effectively prevents metal evaporation.
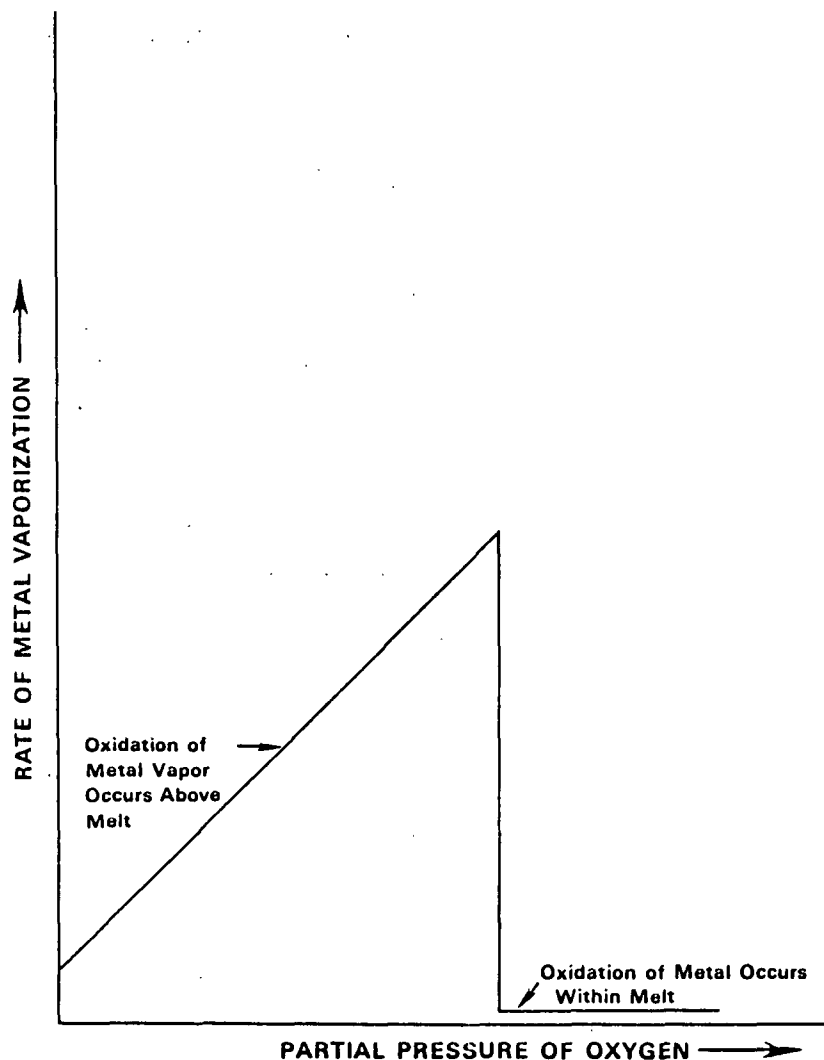
Figure 4. Effect of oxygen on metal vaporization.

MELT CHEMISTRY

The melt in the bed of a recovery furnace consists principally of Na_2CO_3, Na_2S, a few percent Na_2SO_4 and some dispersed carbon. Measurements by Borg et al.[1] and Marriam[9] found the carbon content of the melt to be typically about 5%.

Recent work on carbon oxidation and sulfate reduction[10-12] has shown that carbon oxidation with gaseous O_2 in an alkali carbonate-sulfide melt occurs through a sulfate-sulfide cycle. In this cycle, the carbon is oxidized by Na_2SO_4 to CO_2/CO and the Na_2SO_4 is reduced to Na_2S. The Na_2S is then reoxidized by oxygen to Na_2SO_4, completing the cycle. Experimental results on the burning of kraft char particles have shown that these particles burn through the sulfate/sulfide cycle, with the rate limiting step in this cycle being the reoxidation of Na_2S by O_2. The inorganic molten phase in the particle is mainly Na_2CO_3 and Na_2S.

To understand vaporization from the Na_2CO_3/Na_2S melt in the kraft recovery furnace, it is useful to examine vaporization of Na_2CO_3 melts. Considerable research has been conducted on molten Na_2CO_3 and the sodium oxide compounds present in this melt. Andresen[13] studied Na_2CO_3 melt under partial O_2 atmospheres and concluded that O_2 is present in the melt as peroxide and superoxide, Eq. (14) and (15).

$$Na_2O + 1/2O_{2(g)} \rightleftharpoons Na_2O_2 \qquad (14)$$

$$Na_2O_2 + O_{2(g)} \rightleftharpoons 2NaO_2 \qquad (15)$$
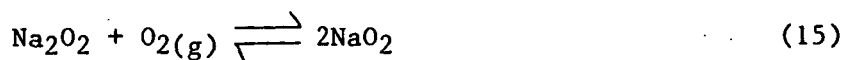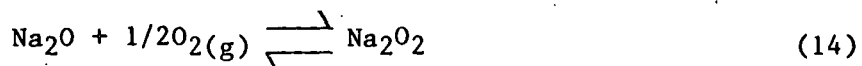
Appleby and Nicholson[14] studied carbonate melts in equilibrium with O_2 and also concluded that these melts predominantly contain peroxide and superoxide in preference to dissolved molecular oxygen.

These studies show that the predominant species present in a Na_2CO_3 melt are Na_2CO_3 and Na_2O. Other sodium oxide species are present but at lower levels. The gas species above a Na_2CO_3 melt are CO_2, O_2 and $Na(v)$.

Theoretical calculations by Brewer and Monstick[15] show that all alkali oxides with the possible exception of Li_2O vaporize to their elements rather than any gaseous molecules. Motzfeld[16] studied the volatilization of Na_2CO_3 and found that the Na_2O concentration at steady state reached a concentration near 1%. Motzfeld[16] concluded that Na_2CO_3 vaporization is described by the following reactions.

$$Na_2CO_3(L) \rightleftharpoons Na_2O(L) + CO_2(g) \qquad (16)$$

$$Na_2O(L) \rightleftharpoons 2Na(g) + 1/2O_2(g) \qquad (17)$$
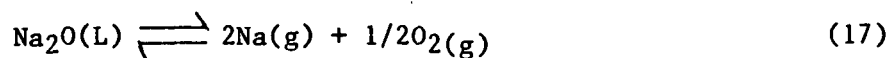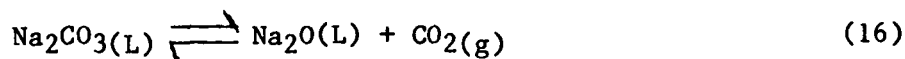
Several researchers have used thermodynamic equilibrium calculations to predict the liquid and gaseous species present in the kraft furnace. Bauer and Doorland[16] were the first to apply this technique to the kraft furnace. Their study predicted that the volatile fuming species in the furnace are Na and Na_2. Sodium hydroxide was considered as a liquid species but not as a gaseous species and was not predicted to be present in the melt.

More recently Warnqvist[2] also applied equilibrium thermodynamics to the kraft furnace and concluded that in addition to Na and Na_2, $NaOH$ is also an important fuming compound. Warnqvist believed that the earlier study by Bauer and Dorland[17] was probably in error for not including $NaOH(g)$ in the equilibrium calculations.

As stated by Warnqvist[2] a major assumption in these equilibrium treatments is that "the waste liquor/air (oxygen) system as a whole comes to chemical

equilibrium." This assumption is recognized to be somewhat unrealistic, but it is felt that this technique provides a hint of the processes and chemical species present in the furnace.

It is unlikely that equilibrium calculations can be used to predict the vaporization rate of a chemical species into a gas with which it is reactive. For example, when determining the vapor pressure of metals by the transpiration technique (a technique where the carrier gas flows over the sample and the vaporization rate is measured by sample weight loss) the carrier gas must be free of any impurities that might react with the metal vapor.[18]

Since furnace gases such as O_2 and CO_2 are reactive with Na and Na_2, equilibrium treatments cannot be used to predict the amount of fume generated through Na and Na_2 vaporization. They can, however, be used to predict the melt composition and the vaporization rate of nonreactive species such as KCl, NaCl, and possibly NaOH.

EXPERIMENTAL SECTION ORGANIZATION

The experimental section of this report is organized into four parts: a description of the experimental apparatus, a study of fume generation during sulfide oxidation, a study of fume generation from other reactions, and a study of the fuming behavior of the nonprocess elements K and Cl. The first section is a description of the experimental apparatus used to study fume generation. The remaining sections contain descriptions of the experiments conducted, the results of these experiments, and discussions of these results.

EXPERIMENTAL APPARATUS

The fume generation experiments were conducted by monitoring the fume produced from alkali carbonate/sulfate/sulfide melts under different atmospheres. The experimental system consisting of an induction heated reactor, gas meters and fume filter is illustrated in Fig. 5. The ceramic reactor was normally charged with approximately 85 g of inorganic salts containing 53 to 80 g of Na_2CO_3, 2.0 to 20 g of Na_2S, and 0 to 40 g of Na_2SO_4.
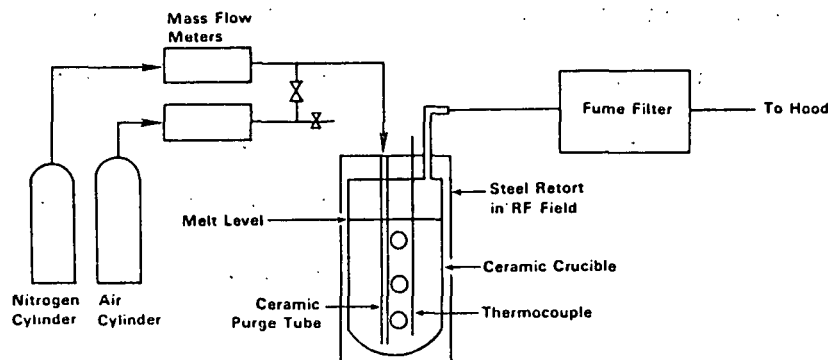
Figure 5. Experimental system.

To ensure that the reagent grade inorganic salts used for this study were anhydrous, they were dried under vacuum (normally for 2 hr at 150°C, except for Na_2S which was dried at 200°C for 24 hr). Analysis of the dehydrated Na_2S revealed that it contained 97 to 98% Na_2S and approximately 1% Na_2SO_4. These salts were then mixed, added to the reactor and rapidly heated under a nitrogen purge to the desired reaction temperature. Approximately 5 to 10 minutes were required to melt the salts and an additional 15 minutes to reach the desired reaction temperature. Once this temperature was reached, O_2 was added to the carrier gas to achieve the desired N_2/O_2 mixture. Essentially no fume was generated as the reagents were heated under the nitrogen purge. To accurately

measure the nitrogen and air flow rates, these gases were metered from pressurized

gas cylinders through thermal mass flowmeters. A mercury manometer in the nitrogen

line monitored the purge pressure and served as a pressure release valve. If

the purge line from the reactor were to become plugged, the mercury in this

manometer would be blown into a vial, releasing the purge pressure and prevent-

ing overpressurization of the reactor.

Two configurations for introducing the purge into the reactor were

employed during this study. These configurations consisted of either introduc-

ing the purge directly into the melt or introducing the purge above the melt.

Figure 4 illustrates the experimental system with the purge introduced below the

melt's surface. With the purge introduced into the melt, the oxygen content of

the purge was totally consumed by sulfide oxidation. With the purge located

above the melt, the sulfide content was oxidized without mixing. This con-

figuration produced a melt with an oxidized surface and also resulted in a

residue of O_2 above the melt. The effect of this residue O_2 partial pressure

was studied by adding different levels of O_2 to the carrier gas.

Two methods of following the rate of fume generation (gravimetric and

flame photometric) were used. The gravimetric consisted of filtering and

weighing the fume particles. The flame photometric consisted of diluting the

fume from the reactor with either air or nitrogen and using a flame photometer

to monitor the sodium content of the off-gas from the reactor.

It was found that the flame photometer output was dependent on the

experimental conditions used to generate fume. The flame photometer responded

differently to fume produced under reducing conditions than to fume produced

under oxidizing conditions. Therefore, the flame photometer was only used with

similar experimental conditions and to ensure that the gravimetric procedure collected all fume particles generated. This was accomplished by monitoring the purge gas from the filter using the flame photometer. Since the gravimetric method produced more accurate experimental data, the results contained in this report were obtained using this procedure.

The effect of the reducing gases, H_2 and CO, was studied by mixing these gases with N_2 and introducing them below the melt's surface. The effects of Cl and K were studied by adding K_2CO_3, NaCl, or KCl to the melt and introducing the N_2 or N_2/O_2 purge below the melt's surface.

FUME GENERATION DURING SULFIDE OXIDATION

The major objective of this study is to define the process or processes responsible for the large quantity of fume generated during sulfide oxidation. This section describes the experiments performed, the experimental results, and based on these results, a mechanism for fume generation under oxidizing conditions.

Of the experimental parameters studied, the mode of gas-melt contact had the most significant effect on fume generation. When sulfide was oxidized with the purge introduced below the melt's surface, large quantities of fume were generated. Although the same rate of sulfide oxidation was achieved with the purge introduced above the melt's surface as with it introduced below the melt's surface, extremely low levels of fume were generated.

The first part of this section describes the effect of the experimental variables (melt composition, temperature, purge rate, surface area and purge O_2 content) on fume generation with the purge introduced below the melt's surface. Next, the effect on fume generation of introducing the purge above the melt is described. Based on these experimental results, a mechanism for fume generation during sulfide oxidation is presented.

FUME ANALYSIS

The fume particles collected during sulfide oxidation were typically white spherical particles approximately 0.25 to 1.0 μm in diameter. Figure 6 is a scanning electron micrograph (SEM) of fume particles collected during sulfide oxidation. Infrared analysis of these fume particles revealed that they are essentially pure Na_2CO_3.
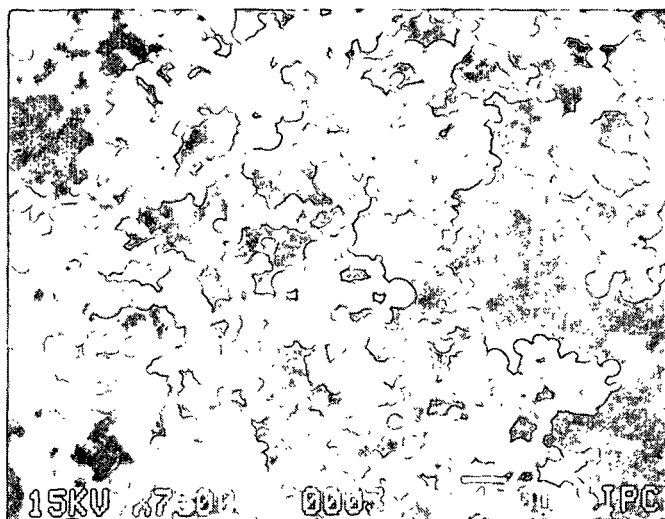
Figure 6. Fume particles collected during sulfide oxidation.

FUME GENERATION WITH PURGE INTRODUCED BELOW THE MELT'S SURFACE

In this section, the effects of sulfide concentration, sulfate concentration, temperature, purge oxygen content, and purge rate on fume generation with the purge introduced into the melt are described.

Typical Experimental Results with Purge Introduced
Below the Melt's Surface

In a typical experiment, the fume generation rate was monitored by filtering the off-gas from the reactor for a five-minute period and weighing the fume collected. Experimental results typical of the majority of the experiments conducted using this procedure are illustrated in Table 1.

As illustrated in this table, the fume generation rate remains at a constant level until the sulfide is nearly totally oxidized. Once the sulfide level reaches a concentration of approximately 0.1 mol/L, the fume generation rate rapidly decreases. Although the relative concentrations of sulfide and sulfate change significantly during this experiment, little change in the fume generation rate is observed until the sulfide is nearly completely oxidized. This indicates that the ratio of sulfide to sulfate has little effect on the fume generation rate.

Table 1. Typical experimental fume generation results with purge
          introduced below the melt's surface

Run 38
Initial Melt Composition   Purge = 1 L/min at 2.1% O_2
Na_2CO_3 = 0.77 mole   Temperature = 927°C (1700°F)
Na_2S = 0.03 mole

Time, s	Calculated Composition		Fume Generation Rate, g/min	Fume Concentration Moles Na_2CO_3 / Mole N_2
	Na_2SO_4, mole/L	Na_2S, mole/L		
755	0.136	0.549	0.0099	0.00214
1280	0.231	0.455	0.0104	0.00224
1760	0.318	0.368	0.0106	0.00288
2240	0.405	0.281	0.0104	0.00224
2721	0.492	0.195	0.0099	0.00214
3114	0.563	0.124	0.0088	0.00190
3639	0.656	0.029	0.0005	0.00011

Effect of Sulfate Concentration

To determine the effect of sulfate level on the rate of fume generation,
the fume generation rate was measured at two different initial levels of sulfate
in the melt. The rate of fume generation was followed using the previously
described gravimetric method, and the results of these experiments are
illustrated in Table 2.

Table 2. Effect of sulfate level on fume generation rate.

Purge Rate = 1.0 L/min at 2.1% O_2, and Temperature = 982°C (1800°F)

Run 39	Run 43
Na_2CO_3 = 0.77 mole	Na_2CO_3 = 0.57 mole
Na_2S = 0.03 mole	Na_2S = 0.03 mole
Na_2SO_4 = 0.00 mole	Na_2SO_4 = 0.30 mole

Time, min	Fume Generation Rate, g/min	Fume Generation Rate, g/min
5	0.0157	0.0125
10	0.0159	0.0127
15	0.0161	0.0121
20	0.0145	0.0149
25	0.0158	0.0103
30		0.0103
35		
Ave.	Std. Dev. 0.0158 ± 0.0006	Std. Dev. 0.0130 ± 0.0019

As illustrated in this table, the level of sulfate in the melt does not significantly affect the fume generation rate. Although the melt in Run 43 contained a high level of sulfate, the fume generation rate was only slightly different from that in Run 39 with no initial sulfate present.

Effect of Sulfide Concentration

To determine the effect of sulfide level on the rate of fume generation, the fume generation rate was measured with different initial levels of sulfide in the melt. The effect of sulfide on the rate of fume generation is shown in Table 3.

Table 3. Effect of sulfide level on fume generation rate.

Conditions: Temperature = 954°C (1750°F)

N$_2$ Flow Rate = 1.0 L/Min

O$_2$ Flow Rate = 0.021 L/min

Na$_2$CO$_3$ mole	Na$_2$S mole	Sulfidity, %	Fume Generation Rate g/min ± Std. Dev.
0.77	0.03	3.7	0.0142 ± 0.001
0.60	0.20	25.0	0.0136 ± 0.001
0.55	0.25	31.0	0.0144 ± 0.001

As illustrated in this table, the level of sulfide has no significant effect on the rate of fume generation.

Effect of Oxygen Partial Pressure on Fume Generation Rate

To determine the effect of oxygen in the purge to the reactor on the rate of fume generation, the oxygen level in the purge was varied. Previous studies of sulfide oxidation with O$_2$/N$_2$ purge introduced below the melt's surface

have shown that essentially all the oxygen supplied to the melt is consumed by
sulfide oxidation. Therefore, to maintain a constant off-gas flow rate from the
melt, the nitrogen level in the purge to the reactor was held constant and the
oxygen level was adjusted. The results of a series of experiments with varying
purge gas oxygen levels are shown in Table 4.

Table 4. Effect of oxygen level in the purge on fume generation rate.

Temperature = 927°C (1700°F)

Run	N_2 L/min	O_2 L/min	Fume Generation Rate, g/min
45	1.02	0.0105	0.00892
46	1.02	0.021	0.0105
47	1.02	0.042	0.0121
48	1.01	0.063	0.0145
49	1.02	0.084	0.0146

As shown in this table, the increase of oxygen in the purge to the
reactor tends to increase the rate of fume generation. However, the fume depen-
dence on the oxygen purge rate is slight. Although the initial level of oxygen
increased by a factor of eight, the fume rate less than doubled.

Temperature Effect

To determine the temperature dependence for fume generation, a number of
gravimetric fume generation rate measurements were made at various temperatures.
Fume generation rates were obtained by oxidizing a $Na_2CO_3-Na_2S$ melt with a 90%
N_2-10% O_2 gas mixture at temperatures ranging from 927 to 1038°C (1700 to 1900°F).

By plotting the ln of the fume generation rate vs. 1/T°K, it was found
that the fume generation had an Arrhenius type temperature dependence with an
activation energy of approximately 20,000 cal/mol, (Fig. 7). At 927°C (1700°F)
the fume generation rate would double for a 108°C (194°F) increase in melt tem-
perature.
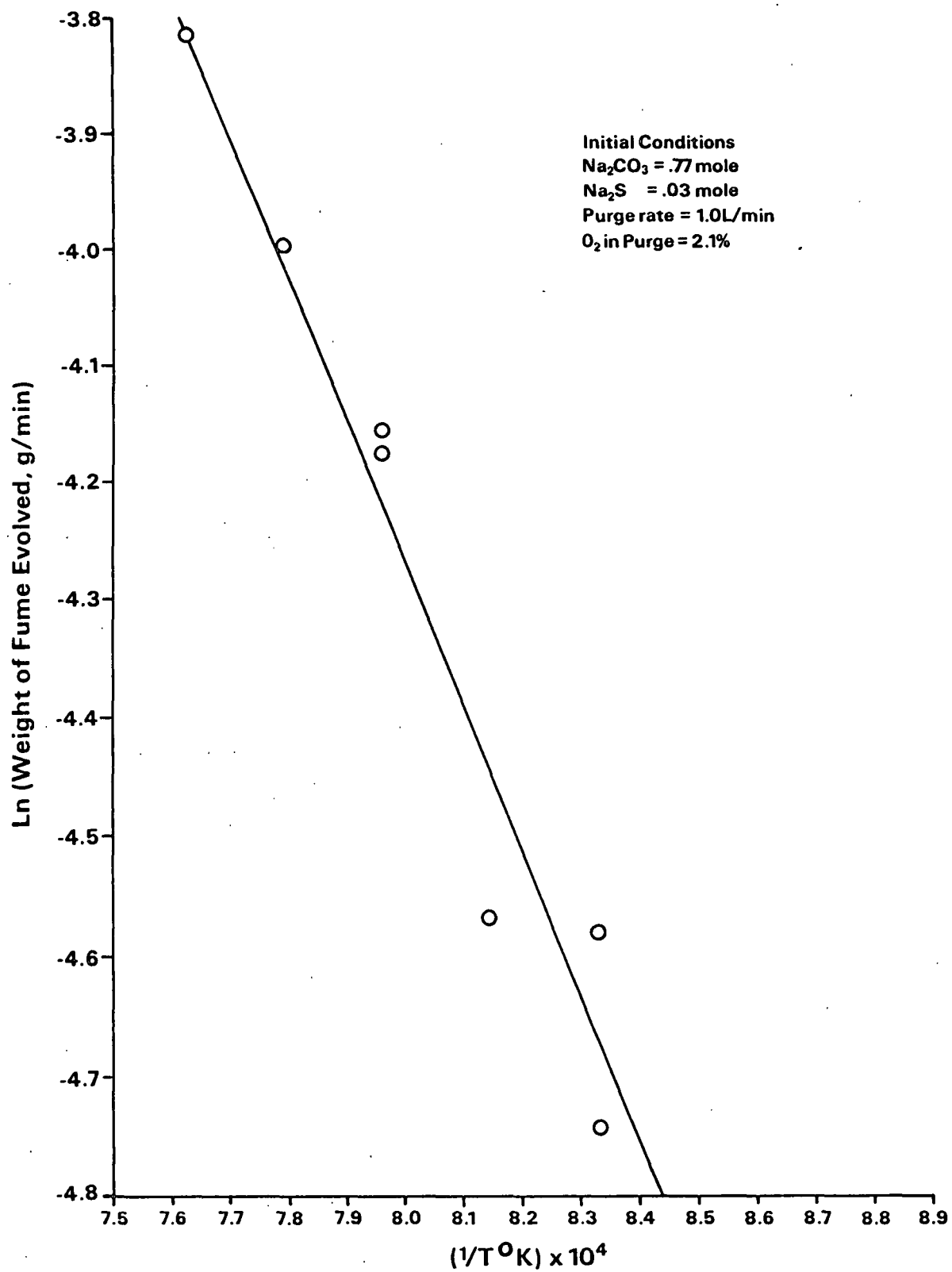
Figure 7. Effect of temperature on fume generation.

Effect of Nitrogen Purge Rate on Fume Generation

To determine the effect of the volumetric purge rate on the fume generation rate, the nitrogen flow rate was varied, while the oxygen flux rate was held constant. Since the oxidation rate is limited by the amount of oxygen supplied, the oxidation rate remained the same for each experiment. The results of these experiments using the gravimetric method of following fume generation are given in Table 5.

Table 5. Effect of purge rate on fume generation.

Initial Melt Conditions: Na_2CO_3 = 0.77 mole
Na_2S = 0.03 mole
Temperature = 927°C (1700°F)

Run	N_2, L/min	Air, L/min	Total N2, L/min	Fume Generation Rate ± Std. Dev., g/min
50	0.04	0.1	0.48	0.00680 ± 0.00032
51	0.6	0.1	0.68	0.00850 ± 0.00076
52	0.8	0.1	0.88	0.01004 ± 0.00042
38	0.9	0.1	0.98	0.01024 ± 0.00032
53	1.06	0.1	1.14	0.01204 ± 0.00042
54	1.23	0.1	1.31	0.01474 ± 0.00198

As seen in Table 5, the fume generation rate is nearly proportional to the volumetric purge rate.

Rate Expression Describing Fume Generation

During sulfide oxidation with the purge introduced below the melt surface a large quantity of Na_2CO_3 fume is generated. The fume generation rate was found to be dependent on the nitrogen and oxygen flow rates to the reactor, and the melt temperature. The sulfate and sulfide concentrations of the melt had little effect on the fume generation rate. Therefore, the fume generation rate was described using the following rate expression.

Rate of Fume Generation, g/min =

$$K(N_2 \text{ Flow Rate, L/min})^M (O_2 \text{ Flow Rate, L/min})^N e^{-\Delta E/RT} \qquad (18)$$

Here K is a constant whose dimensions depend on the values of M and N;

   M and N are powers to which the N_2 and O_2 flow rates are raised; and

   ΔE is the activation energy.

The values of these parameters were determined using a nonlinear regression analysis program and the data from 24 separate experiments. These experiments included a large range of oxygen and nitrogen flow rates and temperatures. Table 6 gives the values of the parameters in Eq. (18).

Table 6. Rate expression describing fume generation from a carbonate melt.

Rate Fume Generation, g/min = $K(N_2, \text{L/min})^M(O_2, \text{L/min})^N e^{-\Delta E/RT}$

Parameter, Value	Linear Estimate of Std. Dev.
K = 161	26
M = 0.907	0.096
N = 0.274	0.024
ΔE = 20,540 cal/mole	1,360 cal/mole

Equation (18) accurately describes the fume generation during sulfide oxidation over a wide range of experimental conditions. One of the more significant findings shown by this equation is the high dependence of the fume generation rate on the nitrogen flow rate relative to the dependence on the oxygen flow rate. The rate of fume generation is almost directly proportional to the nitrogen purge rate into the melt but only proportional to the oxygen purge rate to the 0.27 power.

Effect of Experimental Configuration

   To determine if the reactor configuration or smelt mixing patterns have any affect on fume generation and to confirm the low dependence of the fume

generation rate on the oxygen content of the purge, fume generation during

sulfide oxidation was studied using a larger reactor. This reactor contained

1.5 L of melt (approximately 35 times the amount contained in the smaller reactor)

and was heated by an electric furnace. A purge configuration similar to that of

the smaller reactor system was used with a purge rate of approximately 6 L per

minute (6 times the purge rate used in the smaller reactor). The fume genera-

tion rates obtained with this reactor are shown in Table 7.

Table 7. Effect of oxygen level in the purge on fume generation from
          Marshall Furnace Reactor.

Purge Rate, L/min		% O_2 in Purge	Fume Generation Rate, g/min	Predicted Fume Generation Rate, Eq. (18), g/min
N_2	O_2			
5.61	0.04704	0.827	0.0456	0.073
5.56	0.0941	1.65	0.0639	0.0881
5.31	0.188	3.31	0.0878	0.1021
4.42	1.18	21.0	0.1272	0.143

As shown in this table, the fume generation rates are not highly depen-

dent on the oxygen content of the fume. The fume generation rate was slightly

less than that predicted from Eq. (18). Fume generation remained nearly

constant during this experiment for specific O_2 and N_2 purge rates. This con-

firms that fume generation during sulfide oxidation is independent of the

sulfate and sulfide concentrations in the melt. Since the fuming behavior was

very similar in the two experimental systems, the oxidative fuming rate is not

highly dependent on the reaction system.

Considering the differences in reaction sizes and flow rates, the

fume generation rates in the two systems are very similar. There appeared

to be a greater tendency for fume to deposit on purge lines in the larger

reactor system, which may account for the slightly lower than predicted fuming rates.

Effect of Carbon Dioxide on Fume Generation

One of the major gases present in a kraft recovery furnace is CO_2. In gas samples taken above the bed, Borg[1] found a CO_2 level of 13%.

Since relatively high levels of CO_2 are present in recovery furnaces, the effect of CO_2 on fume generation during sulfide oxidation was studied by monitoring fume generation during sulfide oxidation with various levels of CO_2 added to the O_2-N_2 purge. The effect of different levels of CO_2 in the purge gas on fume generation during sulfide oxidation is shown in Table 8. As illustrated in this table, increasing the level of CO_2 in the purge gas decreases the rate of fume generation.

Table 8. Effect of carbon dioxide on fume generation
          during sulfide oxidation.

$$Na_2CO_3 = 0.77 \text{ mole}$$
Initial Na_2S $= 0.03$ mole
Temp. $= 954°C (1750°F)$

Run No.	N_2 Flow Rate, L/min	O_2 Flow Rate, L/min	CO_2 Flow Rate, L/min	Fume, g/min
107	0.85	0.226	0.00993	0.0129
108	0.826	0.22	0.0157	0.0081
109	0.837	0.223	0.0242	0.0074
110	0.826	0.219	0.0350	0.0064
111	0.861	0.229	0.0767	0.0048
113	0.853	0.227	0.1095	0.0043
120	0.504	0.134	0.292	0.00232

In the experiments shown in Table 8, the CO_2 content of the purge was increased from 1 to 10%. During these experiments the oxygen and nitrogen flow rates were held constant. Since the change in the CO_2 flow rate was small, the total flow rate remained relatively constant. Therefore, the major variable change in these experiments was the CO_2 content of the purge. To determine the effect of CO_2 on the fume, the rate of fume generation was described by Eq. (19).

$$\text{Fume Generation} = K \ P_{CO_2}^N \qquad (19)$$

Here K is a constant,

P_{CO_2} is the mole fraction of CO_2 in the purge, and

N is the power to which the CO_2 mole fraction is raised.

By plotting the log of the fume generation rate against the log of the CO_2 mole fraction in the purge (Fig. 8), n was determined to be -0.48. These results indicate that the fuming rate is inversely proportional to the square root of the CO_2 mole fraction in the purge.

Surface Area Effect

The objective of these experiments was to determine if a change in the surface area of the bubbles would affect the fume generation rate. To increase the melt-gas interface, the single purge tube (0.187 inch ID) was replaced with two purge tubes (0.062 inch ID). To obtain some confidence that this change would produce a significant change in bubble surface area, the change in surface area was estimated using a correlation Eq. (20) for bubble diameter developed by Leibson, et al.[19] This correlation was developed for bubble formation from a single orifice in an air-water system.

$$D_B = 0.18 \ D^{0.5} N_{Re}^{0.33} \qquad (20)$$

Here D_B is the bubble diameter,

D is the orifice diameter, and

N_{Re} is Reynolds number.

This correlation predicts that the previously described change in purge tubes should increase the gas-melt interfacial area in the gas bubbles by approximately 50%. Although this correlation was developed for an air-water system, it does predict a significant increase in interfacial area and it would be reasonable to expect a similar increase in surface area for the gas-melt system used in this study.
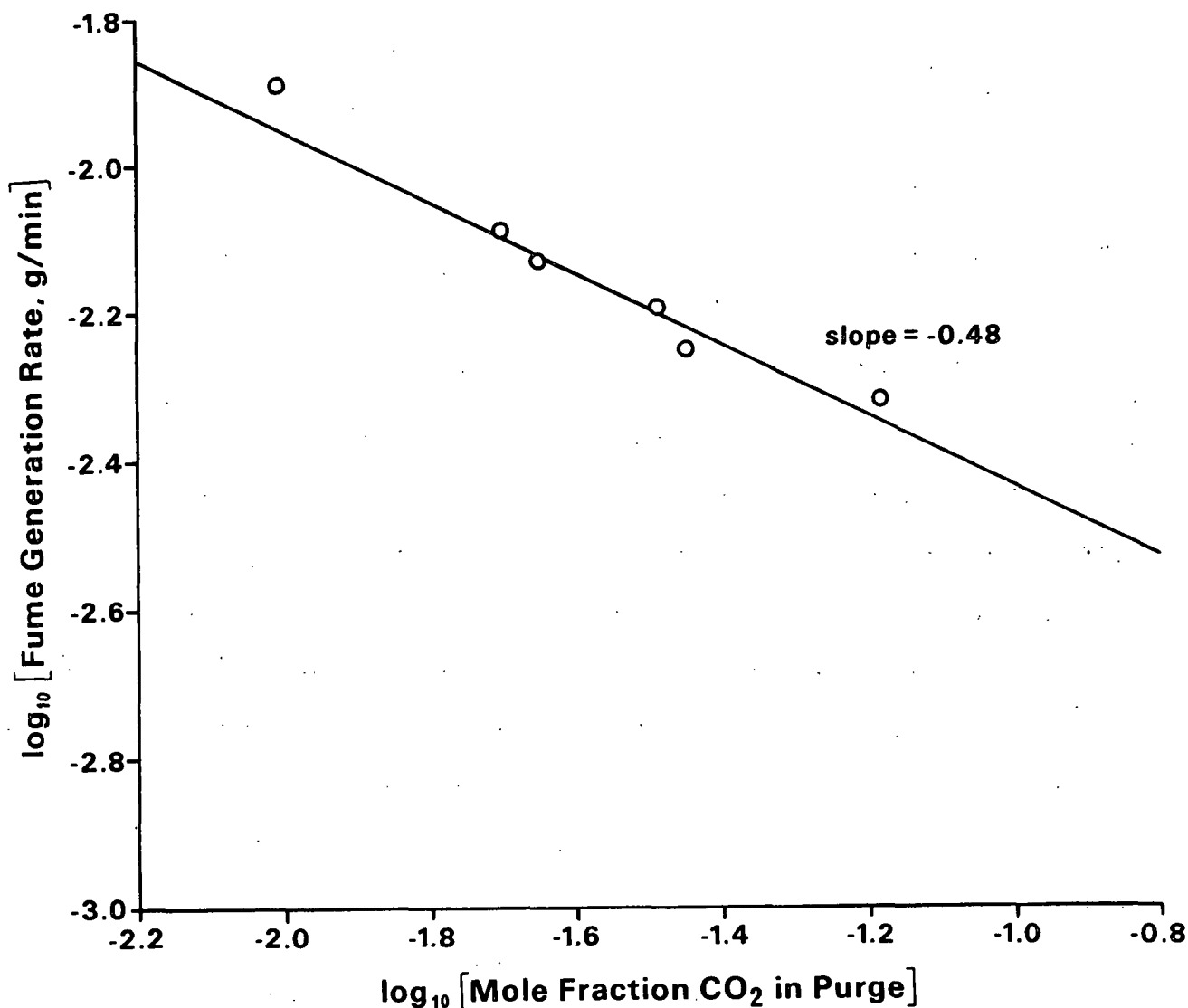
Figure 8. Effect of carbon dioxide on fume generation.

The fume generation rates from several sulfide oxidation experiments employing the two purge tubes are shown in Table 9. Also shown in this table are the predicted fume generation rates using the correlation previously developed for the single purge tube.

Table 9. Effect of two purge tubes on fume generation rate.

Run No.	Temp., °C(°F)	N_2 Flow Rate, L/min	O_2 Flow Rate, L/min	Fuming Rate, g/min ± Std. Dev.	Predicted Fuming Rate, g/min
127	953(1749)	1.03	0.020	0.0129 ± 0.001	0.0126
128	957(1754)	1.03	0.0426	0.0163 ± 0.001	0.0156
129	957(1754)	1.01	0.0634	0.0156 ± 0.001	0.0172

As illustrated in this table, the fume generation rate using the two purge tube system is nearly the same as that predicted for the single purge tube. Therefore, increasing the surface area of the bubbles had little effect on the fume generation rate.

Effect of the Inert Purge Gas on Fume Generation

To determine if the rate limiting step in fume generation during sulfide oxidation is a liquid phase or a gas phase process, the effect of different carrier gases on fume generation was studied. The carrier gas is the inert gas with which the oxygen is mixed. If the controlling process for fume generation during sulfide oxidation is a liquid phase process, the type of carrier gas used should not affect the rate of fume generation. However, if the rate controlling process is a gas phase process, the fume generation rate could be dependent on the type of carrier gas used. Fume generation rates using three different carrier gases are shown in Table 10.

Table 10. Effect of carrier gas on fume generation.

Fume Generation Rates Using N_2, Ar, and He

Conditions: N_2, Ar, He = 1.0 L/min He
            O_2 = 0.01 to 0.20 L/min
            Temperature = 955°C (1750°F)

O_2 Purge Rate, L/min

Gas System	0.01	0.03	0.05	0.10	0.15	0.20
			Fume Generation Rate, g/min			
N_2–O_2	0.0078	0.0128	0.0156	0.0184	0.00232	0.0210
Ar–O_2	0.0086	0.0126	0.0139	0.0168	0.0182	0.0192
He–O_2	0.0053	0.0076	0.0078	0.0093	0.0133	0.0142

With He as the carrier gas, the fume generation rate was significantly lower than the fume generation rates observed with either N_2 or Ar as carrier gas.

FUMING WITH OXYGEN-NITROGEN PURGE
INTRODUCED ABOVE MELT'S SURFACE

To determine the effect of the mode of gas-liquid contact on oxidative fuming, fume generation during sulfide oxidation was studied with the purge located above the melt. Typical fume generation rates during sulfide oxidation using this mode of gas-melt contact are illustrated in Fig. 9 and 10.

Figure 9 illustrates the fume generation rates for low levels of oxygen in the purge. At these rates of oxidation, there isn't much change in the melt composition, and the rate of fume generation remains essentially constant. Figure 10 illustrates the fume generation rates for higher levels of oxygen in the purge. At these rates of oxidation, the rate of fume generation decreases as the sulfide content of the melt is oxidized to sulfate.
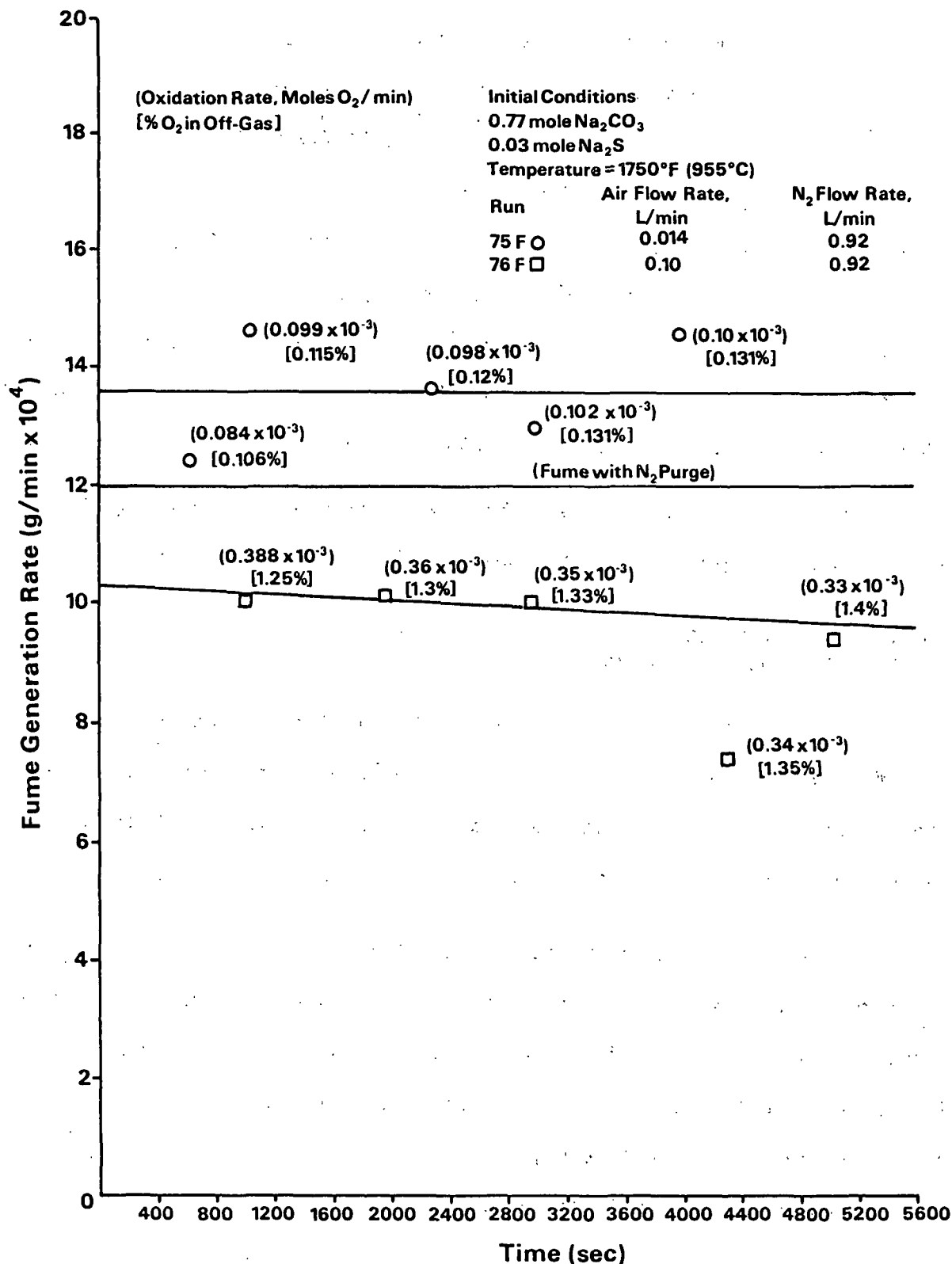
Figure 9. Effect of oxygen on fume generation with purge introduced above melt at low oxygen levels.
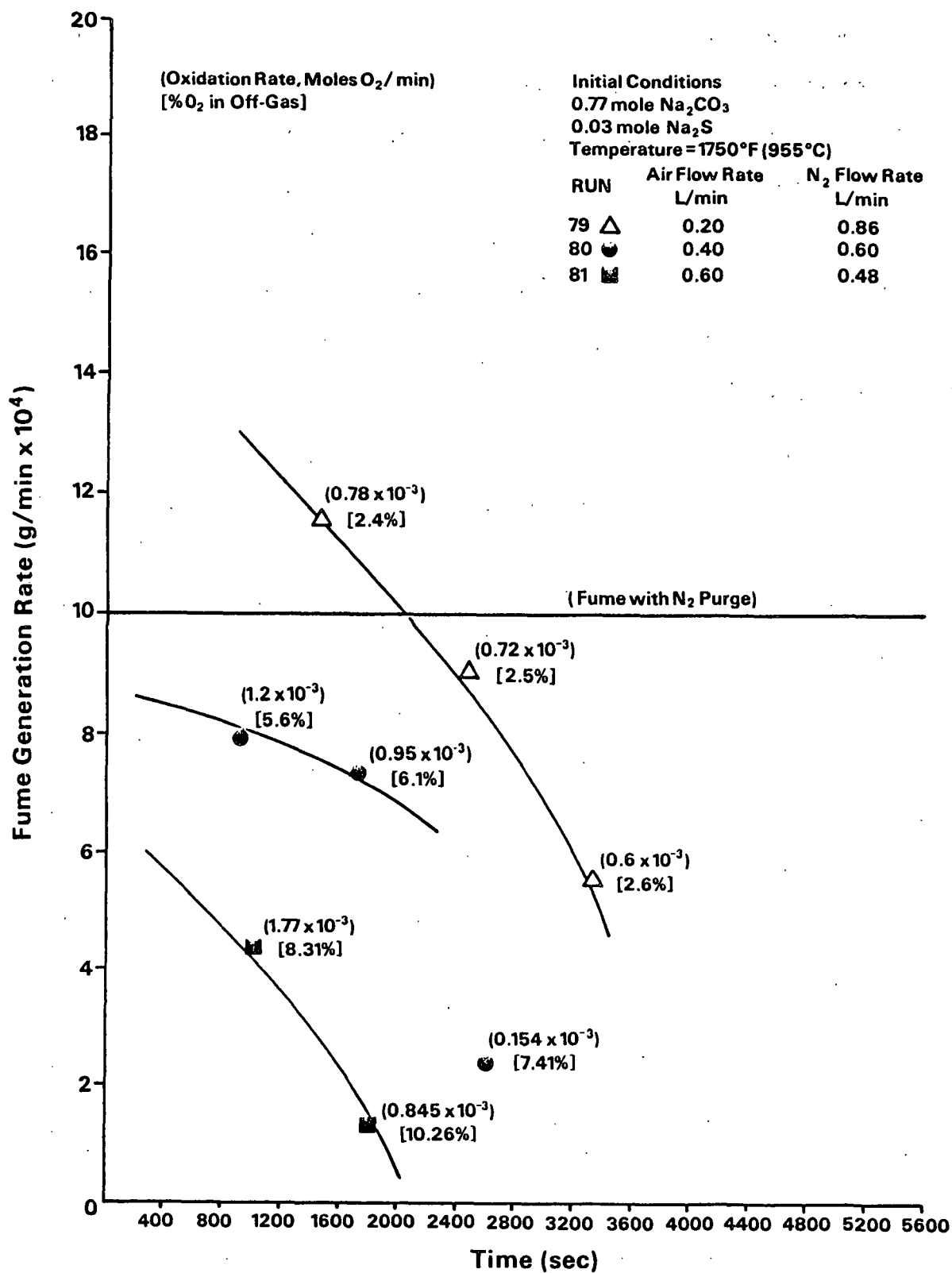
Figure 10. Effect of oxygen on fume generation with purge introduced
            above melt at high oxygen levels.

These figures show that the oxidation of a sulfide in a sulfide-carbonate melt with the oxygen introduced above the melt usually results in a decrease in the fume generation rates compared to that observed under a N_2 purge. Only at extremely low levels of oxygen did the fume generation rate increase. This is in distinct contrast to sulfide oxidation with the purge introduced below the melt surface, where sulfide oxidation produced copious quantities of fume. Also, as the sulfide level in the melt decreased, fume generation rate also decreased. This contrasts to the relatively constant fume generation rate observed with the nitrogen air purge introduced below the melt surface.

In Table 11, the fume generation rates during sulfide oxidation with the purge introduced above the melt's surface are compared to the rates with the purge introduced below the melt's surface. Since the fume generation rate decreased during sulfide oxidation when the purge was introduced above the melt's surface, the fume generation rates in Table 11 for this configuration are the initial rates. Although the same sulfide oxidation rate is achieved in both purge configurations, the fume generation rates with the purge introduced above the melt's surface are approximately an order of magnitude lower than those with the purge introduced below the melt's surface.

Table 11. Effect of purge tube location on fume generation during sulfide oxidation.

Initial Conditions
Na_2CO_3 = 0.77 mole
Na_2S = 0.03 mole
Temperature = 955°C (1750°F)

Purge Introduced Below Melt's Surface		Purge Introduced Above Melt's Surface	
Oxidation Rate, mole O_2 consumed/min x 10^4	Fume Rate, g/min	Oxidation Rate, mole O_2 consumed/min x 10^4	Fume Rate, g/min
9.38	0.0106	0.84	0.00146
9.46	0.0134	3.88	0.00100
		7.80	0.00115
		12.00	0.00079
		17.70	0.00044

The low levels of fume generated with the purge introduced above the melt's surface indicate that the volatile species is oxidized before it evolves from the melt. With the purge introduced below the melt's surface, fresh melt is continually present at the gas-melt interface due to the motion of the bubble rising in the melt. The volatile species then evaporates from the melt and oxidation occurs in the gas phase.

Summary of Experimental Results

The major experimental results obtained in this study are

A) With the purge introduced above the melt's surface, the fume generation rate

    1) was lower under a N_2-O_2 purge than under a pure N_2 purge; and

    2) decreased as the O_2 level in the purge increased.

B) With the purge introduced below the melt's surface, the fume generation rate

    1) was several orders of magnitude greater during sulfide oxidation with a N_2-O_2 purge than under a pure N_2 purge;

    2) was moderately dependent on melt temperature;

    3) was proportional to the N_2 flow rate;

    4) was only slightly dependent on the O_2 content of the purge; and

    5) was independent of bubble size and hence bubble surface area.

DISCUSSION OF FUME GENERATION UNDER OXIDIZING CONDITIONS

The results of this study demonstrate that sulfide oxidation can generate significant quantities of fume. In this section, a mechanism is proposed describing fume generation during sulfide oxidation.

The enhanced fume generation rates observed during sulfide oxidation cannot be considered to be a unique phenomenon. There are many metallurigical processes where the presence of oxygen results in the vaporization of metal oxide fume in much greater quantities than can be accounted for by equilibrium processes. It is also well known that when measuring the vapor pressure of a metal by the transpiration technique one must be certain that the carrier gas is free of any gases that might react with the vapor.[7]

Turkdogan[7] states that there are two possible mechanisms for enhanced vaporization when a melt is exposed to a reactive gas: (1) the formation of a volatile species and (2) the reduction of the mass transfer resistance to evaporization due to the reaction of the volatile species with the reactive gas. In determining the mechanism responsible for fume generation during sulfide oxidation both of these mechanisms were considered.

The effect of the location of the purge tube on fume generation is very similar to the fuming behavior observed with the molten metal systems. The low fuming rate observed with the purge tube located above the melt's surface suggests that the volatile species is oxidized before it can evolve from the melt. The high fuming rate observed with the purge introduced below the melt's surface suggests that the melt at the gas-melt interface is renewed faster than it is oxidized. The volatile species then vaporizes and is oxidized in the gas phase.

This oxidation in the gas phase creates a sink for the volatile species result-ing in an increased rate of vaporization.

Equal rates of sulfide oxidation can be achieved with both modes of gas-melt contact. Therefore, if fume results from the formation of a volatile species during sulfide oxidation, this species should be formed in both modes of gas-melt contact. Since little fume is generated when the purge is introduced above the melt's surface, it is unlikely that fume generation during sulfide oxidation results from the formation of a new volatile compound.

The second critical experiment in the development of the fume genera-tion mechanism is the effect of the inert carrier gas on fume generation. The fuming rate with He as the carrier gas was significantly lower than that with either N_2 or Ar as the carrier gas. This indicates that fume formation is a gas-phase controlled process. It also indicates that this fume is not the result of the formation of new volatile compounds. The formation of such com-pounds would be controlled by liquid-phase processes and the fume generation rate would then be independent of the type of carrier gas used.

Mechanism for Fume Generation under Oxidizing Conditions

Based on the experimental results obtained in this study, the following theory is proposed to explain fume generation during sulfide oxidation. "Fume observed during sulfide oxidation results from the oxidation of Na in the gas phase. This oxidation greatly lowers the partial pressure of Na in the gas phase, increasing Na vaporization from the melt." The presence of Na_2S in the melt is sufficiently reducing to produce a significant Na partial pressure. A detailed description of this fume generation mechanism is presented below.

Liquid Phase Processes

The processes responsible for fume generation during sulfide oxidation can be separated into those processes occurring in the liquid phase and those occurring in the gas phase. In the liquid phase, the concentration of Na in the melt is dependent on the equilibrium, given by Eq. (21).

$$Na_2CO_3 + 1/4\ Na_2S \xrightleftharpoons{K} 1/4\ Na_2SO_4 + 2\ Na + CO_2 \qquad (21)$$
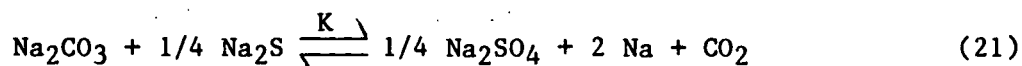
Since the melt used for this study consisted primarily of Na_2CO_3, the activity of Na_2CO_3 is assumed to be approximately 1.0. Then assuming ideal behavior for the Na_2S and Na_2SO_4, the partial pressure for sodium is described by Eq. (22).

$$P_{Na} = \frac{K^{1/2}\ [X_{Na_2S}]^{1/8}}{[X_{Na_2SO_4}]^{1/8}\ [P_{CO_2}]^{1/2}} \qquad (22)$$

Here, P_N is the partial pressure of component N; X_N is the mole fraction of component N; and K is a constant.

Equation (22) indicates that the equilibrium vapor pressure of Na is not highly dependent on the Na_2SO_4 and Na_2S concentrations in the melt. This explains why changes in the Na_2SO_4 and Na_2S concentrations have little effect on the fume generation rate until only a very low concentration of Na_2S remains in the melt.

Fume generation was previously found to be inversely proportional to the square root of the CO_2 partial pressure. Assuming that the fume generation rate is dependent on the equilibrium partial pressure of Na, it is interesting to note that this effect of CO_2 on the fume generation rate is predicted by Eq. (22).

Gas Phase Processes

The most significant process occurring in the gas phase is the oxidation of Na, which lowers the partial pressure of Na in the gas. Since the rate of Na vaporization depends on the difference between the vapor pressure of Na at the melt-gas interface and the partial pressure in the gas, the reduction in partial pressure increases the vaporization of Na.

The reactions occurring in the gas phase are represented by Eq. (23) and Eq. (24).

$$2 \ Na + 1/2 O_2 \rightleftharpoons Na_2O \tag{23}$$

$$Na_2O + CO_2 \rightleftharpoons Na_2CO_3 \tag{24}$$

These equations are not intended to represent a mechanism, but are intended to indicate the stoichiometry of the gas phase reactions.

The consumption of CO_2 in the gas also increases the rate of Na vaporization. If only Na was consumed in the gas phase reactions, the CO_2 generated would shift the equilibrium represented by Eq. (21) toward the left and result in a lower vapor pressure for Na.

Fume Generation under Oxidizing Conditions

The liquid and gas phase processes occurring during oxidative fuming are illustrated in Fig. 11.

In this figure, Na and CO_2 are generated in the melt from the equilibrium reaction between Na_2CO_3 and Na_2S, as given by Eq. (21). The Na and CO_2 then evaporate and react with O_2 diffusing toward the melt at some distance δ from the melt.

O_2 flux

Gas   Phase
$\frac{1}{2}O_2 + CO_2 + 2Na \longrightarrow Na_2CO_3$ (fume)

δ $\uparrow Na, CO_2$ flux

Gas—Melt
Interface

Liquid Phase

$Na_2CO_3 + \frac{1}{4}Na_2S \rightleftharpoons \frac{1}{4}Na_2SO_4 + CO_2 + 2Na$
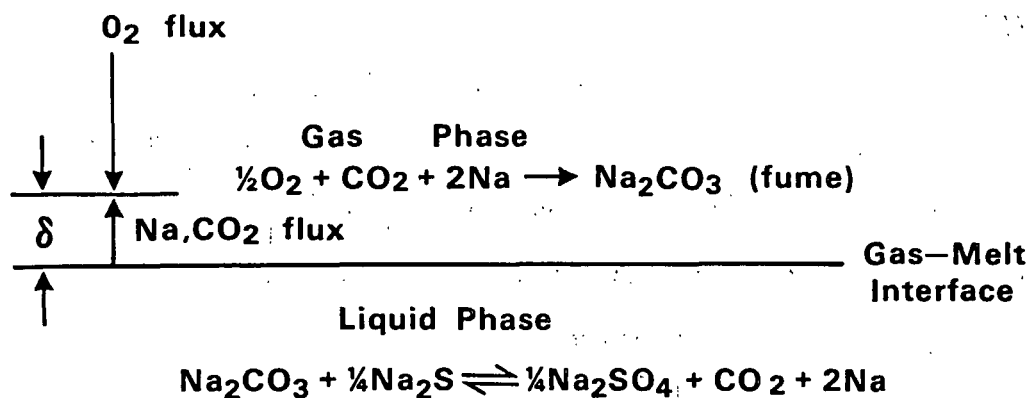
Figure 11. Fume generation under oxidizing conditions.

Applying the film theory for mass transfer to this system, the rate of Na vaporization is described by Eq. (25).

$$Jm = \frac{D_{Na}}{\delta \ RT} (P_{Na}^* - P_{Na}) \quad \text{moles/cm}^2\text{-s} \tag{25}$$

Here, Jm is the Na flux from the melt;

D_{Na} is the diffusivity of Na in the gas;

δ is the distance from the surface where the oxidation of Na occurs;

R is the ideal gas constant;

T is the absolute temperature;

P_{Na}^* is the vapor pressure of Na at the gas—melt interface; and

P_{Na} is partial pressure of Na at distance δ.

Since $P_{Na}^* \gg P_{Na}$, Eq. (25) can be written as

$$Jm = \frac{D_{Na}}{\delta \ RT} P_{Na}^* \tag{26}$$

As the partial pressure of O_2 is increased, the distance δ from the melt where fume is formed decreases and the rate of fume generation increases. As in the case for the molten metals, O_2 eventually penetrates to the melt's surface. The Na_2S and Na in the melt are then oxidized, reducing the vapor pressure of Na ($P_{Na}*$). Once oxidation occurs in the melt, the fume generation rate is significantly reduced due to the low vapor pressure of Na.

APPLICATION OF FUME GENERATION THEORY
TO THE EXPERIMERNTAL RESULTS

Described below is the application of the proposed fume generation theory to the two modes of gas–melt contact used during this study. In one mode of gas–melt contact, the O_2-N_2 purge was introduced above a relatively quiescent melt. With this mode of oxidation, little fume was observed and the rate of fume generation decreased as the O_2 partial pressure was increased.

In the other mode of gas–melt contact, the O_2-N_2 purge was introduced below the melt's surface. This mode of oxidation generated a high level of fume. Although the fume generation rate was not highly dependent on the O_2 content of the purge, the fume generation rate increased as the O_2 content of the purge increased.

Interpretation of Fume Generation with Purge
Introduced above Melt's Surface

With the purge introduced above the melt, relatively little fume was generated during sulfide oxidation. Only at extremely low O_2 partial pressures was the fume generation during sulfide oxidation greater than that produced with a pure N_2 purge.

The fume generation behavior observed with the purge introduced above the melt is very similar to that reported in Turkdogan's study[6] of fuming during

the oxidation of molten metals. At low O_2 partial pressure, the Na evolving

from the melt is oxidized above the melt, lowering the partial pressure of Na

and increasing the rate of Na vaporization.

At higher O_2 partial pressures, the O_2 penetrates to the melt surface.

Oxidation of the Na and Na_2S then occurs in the melt and little fume is generated.

The vapor pressure of Na above a $Na_2S-Na_2CO_3$ melt is relatively low

compared to the vapor pressure of the metals. The O_2 partial pressure required

to penetrate the boundary layer to the melt surface is also relatively low for

Na in the $Na_2S-Na_2CO_3$ melts compared to the metal systems. Therefore, with the

purge introduced above the melt, an increase in fume generation is observed only

at low O_2 partial pressures. While in the metals systems, an increase in fume

generation occurs even at relatively high O_2 partial pressures.

Interpretation of Fume Generation with Purge Introduced below Melt's Surface

The fuming behavior during sulfide oxidation with the purge introduced

below the melt's surface was considerably different than that observed with the

purge introduced above the melt. The major difference was the high level of

fuming during Na_2S oxidation with the purge introduced below the melt's surface.

The effect of O_2 partial pressure was also significantly different in the two

modes of gas-melt contact. With the purge introduced below the melt's surface,

increasing the O_2 partial pressure in the purge resulted in a slight increase

in the rate of fume generation. This contrasts to the decrease in fume genera-

tion with an increase in O_2 partial pressure when the purge was introduced above

the melt. The Na_2S level in the melt also produced different effects on the

rate of fuming in the two modes on melt-gas contact. With the purge introduced

above the melt, fuming rate decreased as the Na_2S was oxidized to Na_2SO_4. With

the purge introduced below the melt's surface, the level of Na₂S had no effect

on the fuming rate until only low levels of Na₂S remained in the melt.

With the purge introduced below the melt's surface, fume is generated

in the bubble as it rises in the melt (Fig. 12). The liquid surrounding the

bubble is continually renewed, and due to the liquid flowing past the bubble the

gas in the bubble may undergo toroidal circulation. The basic difference be-

tween this mode of oxidation and oxidation with the purge introduced above the

melt is the mixing of the liquid at the gas-melt interface.
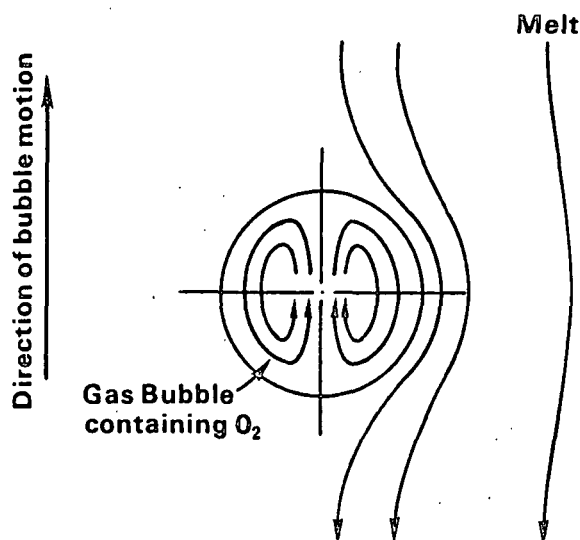
Figure 12. Fume generation in a rising gas bubble.

In a gas-liquid reaction, the reaction rate may be limited by (A) gas

side mass transfer, (B) liquid side mass transfer, (C) the chemical kinetics, or

(D) a combination of these processes. Since the oxidation of Na₂S in a car-

bonate melt is an extremely fast reaction, it is possible that this reaction is

mass transfer limited. When the purge tube was introduced above the melt's sur-

face, only low levels of fume were observed during sulfide oxidation. In this

mode of oxidation, the reaction is limited by liquid side mass transfer.

Since copious amounts of fume were generated during sulfide oxidation when the purge was introduced below the melt's surface, the melt at the liquid-gas interface is unoxidized in this mode of sulfide oxidation. The sulfide oxidation reaction is then limited by either gas side mass transfer or by chemical kinetics. If kinetics limits the oxidation rate, the majority of the chemical species in the melt at the interface should be oxidized and the fraction of oxidized species should be dependent on the O_2 partial pressure in the purge gas. This situation would be similar to that with the purge tube introduced above the melt. The fume generation rate should be low and should decrease as the O_2 partial pressure in the gas is increased. Since a high level of fume was present and the fuming rate increases with an increase in O_2 partial pressure, the oxidation rate is not kinetically limited, but is likely gas-phase mass transfer limited.

The effect of different carrier gases on the fume generation rate, Table 10, also indicates that the sulfide oxidation rate is not limited by the chemical kinetics. Helium, the carrier gas in which the diffusivities are the highest, produced the lowest fuming rate. If the Na_2S oxidation reaction was limited by the chemical kinetics, the carrier gas would not affect the reaction rate. The vapor pressure of the volatile species would not be affected by the carrier gas and the only effect the carrier gas would have would be on the rate of flux of the volatile species from the surface. Carrier gases with higher diffusivities such as He would have higher fluxes of the volatile species and would produce higher fuming rates. Since He produced the lowest fuming rate, the reaction rate and fume generation process are not limited by the chemical kinetics.

As the gas bubble rises in the melt, the melt at the interface is constantly mixed. This mixing of the melt and the fast rate of the oxidation reaction results in the reaction being controlled by gas side mass transfer. Figure 13 illustrates the relative O_2, Na, and Na_2S concentrations at the interface during Na_2S oxidation.
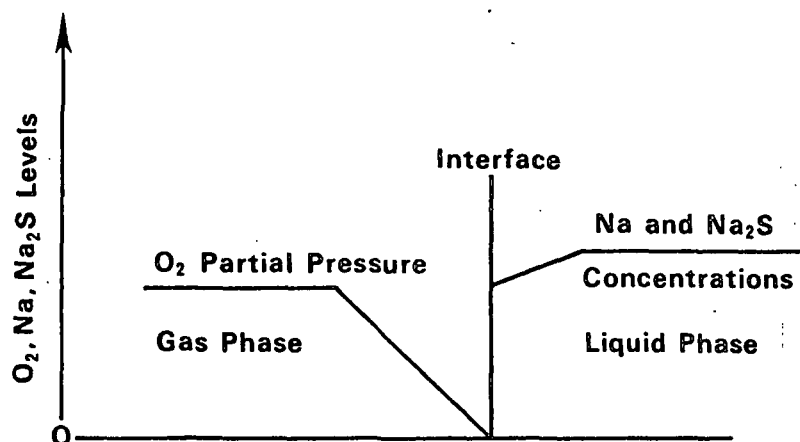
Figure 13.   Relative levels of O_2, Na, and Na_2S at bubble interface during sulfide oxidation.

The O_2 partial pressure in the gas falls to near zero at the interface. Since the melt is renewed at the interface faster than it is oxidized, the Na and Na_2S concentrations at the interface are nearly identical to those in the bulk melt.

In this situation, Na evolves from the melt and is oxidized near the interface in the gas. This oxidation lowers the partial pressure of Na in the gas and significantly enhances the rate of Na evolution. The fume generation rate is constant as long as sufficient O_2 remains in the gas to oxidize the Na evolving from the melt. The fume generation rate observed then depends on the time required for consumption of the O_2 in the bubble.

The rate of O_2 consumption is described by Eq. (27).

$$\frac{d(N_{O_2})}{dt} = S\ Kg\ (P_{O_2} - P_{O_2}{}^*) \tag{27}$$

Here, P_{O_2} is the partial pressure of O_2 in the bulk gas;

$P_{O_2}{}^*$ is the partial pressure at the interface;

Kg is the gas phase mass transfer coefficient

N_{O_2} is moles of O_2; and

S is interfacial surface area

Since $P_{O_2} \gg P_{O_2}{}^*$, Eq. (28) can be written as:

$$\frac{d(N_{O_2})}{dt} = S\ Kg\ P_{O_2} \tag{28}$$

The partial pressure of O_2 in the gas is shown in Eq. (29):

$$P_{O_2} = \frac{N_{O_2}}{N_{N_2} + N_{O_2}} \times Pt \tag{29}$$

Here, Pt is the total pressure.

For the experimental conditions used in this study the O_2 content in the gas during sulfide oxidation is much less than the N_2 content of the gas. The partial pressure of O_2 is then approximated by Eq. (30).

$$P_{O_2} = \frac{N_{O_2}}{N_{N_2}}\ Pt \tag{30}$$

The rate of O_2 consumption is then given by Eq. (31)

$$\frac{d(N_{O_2})}{dt} = S\ Pt\ Kg\ \frac{N_{O_2}}{N_{N_2}} \tag{31}$$

During sulfide oxidation, the fume generation rate remains constant until the O_2 level in the gas bubble falls below that required to rapidly oxidize the Na being evolved. The weight loss of the melt due to fuming (or fume generated during this period) is then described by Eq. (32).

$$\frac{dF}{dt} = - K S \qquad (32)$$

Here, F is the weight of material evolved from the melt during the fuming period, and K is a constant.

Dividing Eq. (32) by Eq. (31) gives the change in fume with the O_2 content of the gas bubble, Eq. (33)

$$\frac{d\ F}{d\ (N_{O_2})} = - \frac{K}{Kg\ Pt} \frac{N_{N_2}}{N_{O_2}} \qquad (33)$$

Once the O_2 level in the bubble falls to the level where the Na evolved is not oxidized, fume generation essentially stops. Equation (33) can then be integrated between the following boundary conditions.

1) For initial moles of O_2 in bubble ($N_{O_2 I}$), fume generation
   (F) = 0.

2) For finial moles O_2 in bubble ($N_{O_2 F}$), fume generated = total fume (Ft).

$$\int_{o}^{Ft} dF = - \frac{K\ N_{N_2}}{kg\ Pt} \int_{N_{O_2 I}}^{N_{O_2 F}} \frac{dN_{O_2}}{N_{O_2}} \qquad (34)$$

$$Ft = \frac{K\ N_{N_2}}{Kg\ Pt} [\ln\ (N_{O_2 I}) - \ln\ (N_{O_2 F})] \qquad (35)$$

To test this model of fume generation, the fume generation rates were plotted vs. the ln of the initial O_2 flow rates, Fig. (14), for the three different carrier gases in Table 12. From Eq. (35), this plot of the ln of the initial O_2 molar flow rates vs. the fume generation rate should yield a straight line.

As illustrated in Fig. 14, Eq. (35) accurately describes the effect of O_2 on fume generation during sulfide oxidation with the purge introduced below the melt's surface. In Fig. 14, fume generation for O_2 in N_2 and Ar is clearly a logarithmic function of the initial O_2 content of the purge. The logarithmic dependence is less clear for O_2 in He, but this is likely due to scatter in the data.

The lower fume generation rate in He is due to O_2 having a higher diffusivity in He than it has in either Ar or N_2. This higher diffusivity results in faster consumption of the O_2 and hence a shorter time for fume generation.

The penetration theory first proposed by Higbie[20] predicts that the mass transfer coefficient should be proportional to the square root of the diffusivity, as given by Eq. (37).

$$K_A \propto D_A^{1/2} \tag{37}$$

Then from Eq. (35), the fume generated as the bubble passes through the melt should be inversely proportional to the square root of the interdiffusivity of O_2 in the carrier gas.

To confirm this, the diffusivities for O_2 in the three inert carrier gases were calculated using the Wilke and Lee[21] modification of the equation by Hirschfelder, Bird and Spotz.[22]
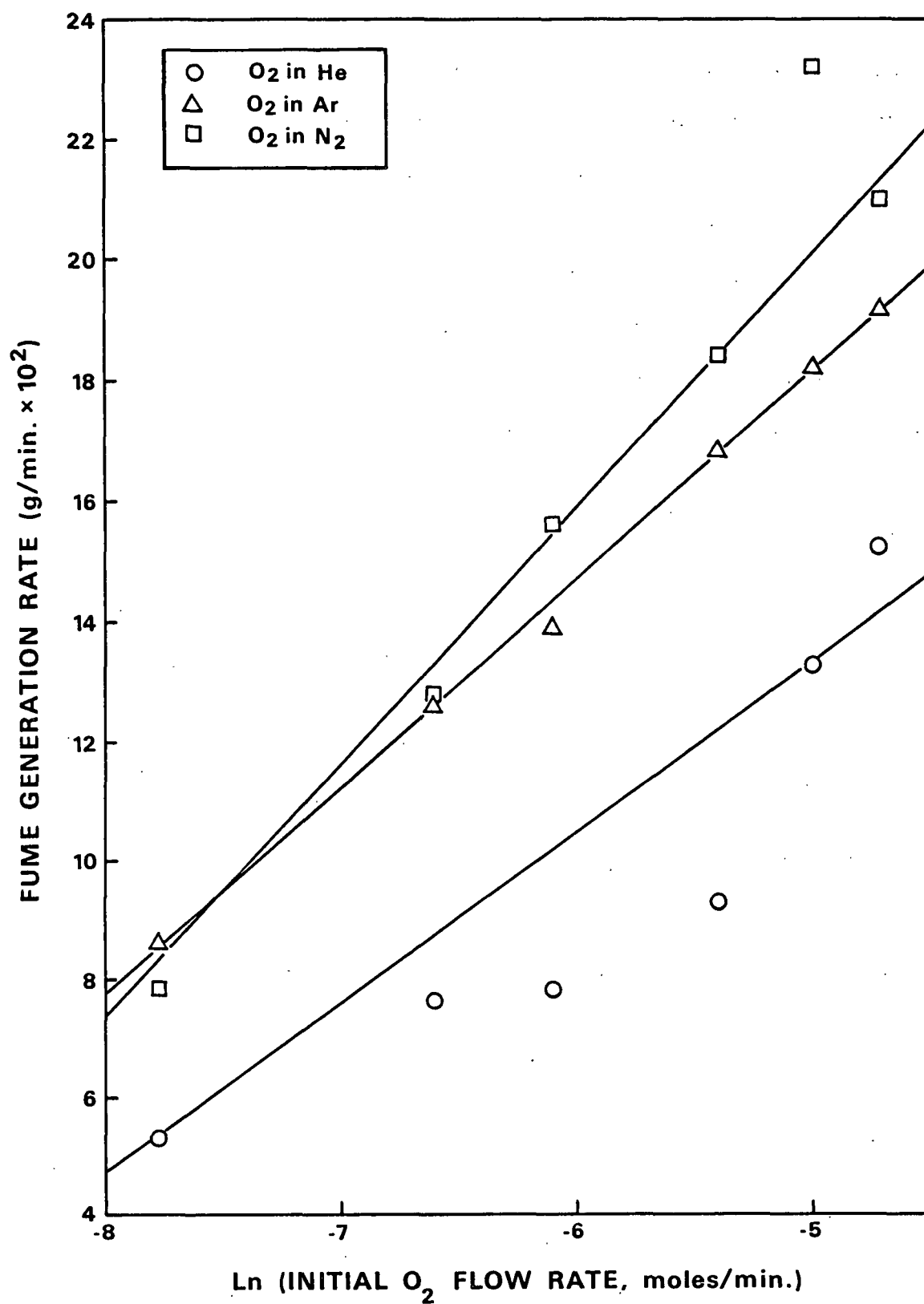
Figure 14.   Effect of O_2 on fume generation in N_2, Ar, and He.

Table 12 lists the calculated diffusivities of O_2 in the three carrier gases used in this study, the predicted fuming rates relative to the N_2-O_2 system, and the actual fuming rates relative to the N_2-O_2 system. The actual relative fuming rates in this table are the average of the fuming rates of the different O_2 levels relative to the N_2-O_2 system. The predicted relative fuming rates are based on the change in the gas mass transfer coefficient resulting from changes in the diffusivities of O_2 in the carrier gases. As shown in this table, the actual relative fuming rates are quite close to those predicted on the basis of changes in O_2 diffusivities in the carrier gases.

Table 12. Effect of gas diffusivity of fume generation.

Gas System	Diffusivity ± Av. Error, cm^2/s	Predicted Relative to N_2-O_2 Fuming Rates, g/min	Actual Relative to N_2-O_2 Fuming Rates ± 1 Std. Dev., g/min
N_2-O_2	2.44 ± 0.1	1.0	1.0
$Ar-O_2$	2.38 ± 0.1	1.01	0.93 ± 0.10
$He-O_2$	8.08 ± 0.3	0.55	0.58 ± 0.07

This mechanism for oxidative fuming accurately explains the effects of the experimental variables on fume generation during sulfide oxidation. The major effects of the experimental variables on fume generation and their relationship to the proposed mechanism are summarized below.

(A) Fume generation during sulfide oxidation with the N_2-O_2 purge introduced above melt's surface.

    1. Fume generation with a N_2-O_2 purge was normally less than that under a N_2 purge. This results from the sulfide oxidation rate being liquid side mass

transfer limited in this mode of gas-melt contact.

The melt at the gas-melt interface is oxidized and

the vapor pressure of Na is low in this oxidized state.

2. Only at very low O_2 partial pressures was the fume

generation rate greater than that present with a N_2

atmosphere. This results from low O_2 partial pressures

not being sufficient to oxidize the melt's surface.

Sodium then vaporizes from the melt and is oxidized

in the gas above the melt. This creates a Na

sink and increases the rate of Na vaporization.

(B) Fume generation during sulfide oxidation with the N_2-O_2 purge introduced

below the melt's surface.

1. Sulfide oxidation in this mode of gas-melt contact

produces large quantities of fume. This results

from sulfide oxidation being gas side mass transfer

limited. The melt at the gas-melt interface has a rela-

tively high level of Na. As soon as this Na evolves

from the melt it is oxidized in the gas phase. This

oxidation lowers the partial pressure of the Na and

increases the vaporization rate.

2. The rate of fuming is nearly proportional to the N_2

purge rate. This results from the rate of oxygen

consumption in the gas bubble being inversely proportional

to the N_2 purge rate, Eq. (31). Therefore, as the N_2

purge rate increases, the time required for complete

consumption of the O_2 in the purge is also increased and more fume is generated.

3. The fume generation rate depends logarithmically on the O_2 content of the purge. This results from the rate of consumption of O_2 in the gas bubble being proportional to the O_2 concentration. The rate of O_2 consumption is then a logarithmic function. This logarithmic dependence of the fuming rate is predicted by Eq. (35).

4. The bubble size and hence surface area had no effect on the fume generation rate. This results from the rate of sulfide oxidation, Eq. (31), and the rate of fume generation, Eq. (32), both being directly proportional to the surface area. Since the surface area drops out when these equations are combined, Eq. (33), the surface area of the gas bubble does not affect the fume generation rate.

5. Fume generation during sulfide oxidation is not dependent on the Na_2SO_4 and Na_2S content of the melt. This results from the low Na dependence on these compounds, Eq. (22).

6. Carrier gases with higher O_2 interdiffusivities produce lower fume generation rates. This results from higher interdiffusivities producing faster rates of O_2 consumption. Since the O_2 in the bubble is consumed faster, fuming lasts for a shorter period of time and less fume is produced.

FUME GENERATION UNDER REDUCING CONDITIONS

This section presents an experimental study of fume generation under reducing conditions. The reducing conditions studied included the effect of the presence of H_2 and CO in the gas phase and the effect of the presence of carbon (kraft char) in the melt.

CARBON MONOXIDE

To determine if CO reduction of Na_2CO_3, Eq. (38) is a mechanism for fume generation, CO (1 to 10%) was added to the purge gas. The effect of CO on fume generation in Na_2CO_3-Na_2S melts with and without Na_2SO_4 present is shown in Table 13.

$$CO + Na_2CO_3 \longrightarrow 2\ CO_2 + 2\ Na(v) \qquad (38)$$
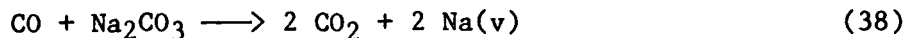
Table 13. Effect of carbon monoxide on fume generation.

Temp., °C	Melt Composition			Purge Rate		Fume Generation, g/min
	Na_2CO_3, mole	Na_2S, mole	Na_2SO_4, mole	N_2, L/min	CO, L/min	
954[a]	0.77	0.03	0	1.0	0	0.00076
954	0.77	0.03	0	0.98	0.01	0.00036
954	0.77	0.03	0	0.98	0.03	0.00076
954	0.77	0.03	0	0.98	0.05	0.00080
954	0.77	0.03	0	0.95	0.10	0.00072
954	0.77	0.03	0.01	0.98	0.10	0.00000
954	0.77	0.03	0.02	0.98	0.10	0.00016

[a]Pure N_2 purge.

As shown in this table, the addition of CO to the purge did not result in an increase in fume generation over a pure N_2 purge. With Na_2SO_4 present in the melt, little or no fume was observed with CO present in the purge gas. Therefore, CO reduction of Na_2CO_3 is not a major mechanism for fume generation.

HYDROGEN

To determine if H_2 reduction of Na_2CO_3, Eq. (39), results in signifi-
cant fume, this reaction was studied by purging Na_2CO_3-Na_2S melts with H_2/N_2 gas
mixtures. The H_2 level in the purge was varied from 2 to 10%. The fume genera-
tion rates resulting from the presence of H_2 in the purge are shown in Table 14.

$$Na_2CO_3 + H_2 \longrightarrow 2Na + CO_2 + H_2O \qquad (39)$$
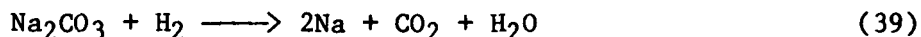
Table 14. Effect of hydrogen on fume generation.

Temp., °C	Melt Composition			Purge Rate		Fume Generation, g/min
	Na_2CO_3, mole	Na_2S, mole	Na_2SO_4, mole	N_2, L/min	H_2, L/min	
954[a]	0.77	0.03	0	1.0	0	0.00076
955	0.77	0.03	--	0.92	0.02	0.0007
955	0.77	0.03	--	0.92	0.05	0.0008
955	0.77	0.03	--	0.92	0.10	0.002
955	0.77	0.03	0.03	0.92	0.10	0.002

[a]Pure N_2 purge.

Although the rate of fume generation in the presence of H_2 is greater
than that observed with CO, it is significantly lower than the typical levels
observed during oxidative fuming. For example, air oxidation of the melts in
Table 14 would produce an order of magnitude more fume than was produced with H_2.

CARBON

To determine if the reduction of Na_2CO_3 with carbon, Eq. (40), is a major
mechanism for fume generation, the rate of fume generation was measured with
kraft and soda char present in Na_2CO_3-Na_2S melts. The fume generation rates
were measured under both N_2 and N_2-O_2 purges and are shown in Table 15.

$$2 \ C + Na_2CO_3 \longrightarrow 2 \ Na(v) + 3 \ CO \qquad (40)$$
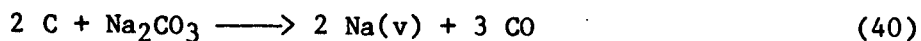
Table 15. Effect of carbon on fume generation.

| Temp., °C | Melt Composition | | | Purge Rate | | Fume Generation, g/min |
	Na_2CO_3, mole	Na_2S, mole	Carbon Content mole	N_2, L/min	O_2, L/min	
954[a]	0.77	0.03	0.0	1.0	0	0.00076
954	0.77	0.03	0.016,S	0.92	0	0.0012
954	0.77	0.03	0.016,S	1.08	0.042	0.0162
954	0.77	0.03	0.032,S	0.92	0	0.0039
954	0.77	0.03	0.032,S	1.08	0.042	0.015
954	0.77	0.03	0.016,K	0.92	0	0.002
954	0.77	0.03	0.016,K	1.08	0.042	0.0155
954	0.77	0.03	0.032,K	0.92	0	0.0025
954	0.77	0.03	0.032,K	1.08	0.042	0.0163

S = Carbon from soda char, K = carbon from K char.
[a]Pure N_2 purge, no carbon present in melt.

At the carbon levels used in these melts, the fume generation rate due to the reaction of carbon with Na_2CO_3 is approximately an order of magnitude lower than the fume produced with the addition of oxygen to the purge.

Relative to fuming during sulfide oxidation, the reductive mechanisms produced only a small level of fume. The presence of CO in the purge gas did not produce a detectable increase in the rate of fume generation over a pure N_2 purge. Although H_2 and C did produce more fume than a pure N_2 purge, their fume generation rates were significantly lower than those observed during sulfide oxidation.

SODIUM HYDROXIDE EFFECT

One of the proposed mechanisms for fume generation is the formation and vaporization of NaOH. To determine if NaOH is a major source of fume, NaOH pellets were added to Na_2CO_3-Na_2S melts and the fuming rates were measured under N_2 and N_2-O_2 purges. Table 16 lists the fume generation rates from melts containing different levels of NaOH. Also shown in this table is the fume generation rate during sulfide oxidation with no NaOH present.

Table 16. Effect of NaOH on fume generation.

Temp., °C	Melt Composition			Purge Rate		Fume Generation, g/min
	Na_2CO_3, mole	Na_2S, mole	NaOH, mole	O_2, L/min	N_2, L/min	
954[a]	0.77	0.03	0	0	1.0	0.00076
955[b]	0.77	0.03	0.0	0.021	1.0	0.013
955	0.77	0	0.012	0	1.0	0.0000
955	0.77	0	0.031	0	1.0	0.00006
955	0.77	0.03	0.010	0	1.0	0.0007
955	0.77	0.03	0.10	0	1.0	0.0007
955	0.77	0.03	0.03	0.021	1.0	0.0048
955	0.77	0.03	0.06	0.021	1.0	0.0015

[a]No NaOH present in melt under N_2 purge.
[b]No NaOH present in the melt under N_2-O_2 purge.

As illustrated in this table, the addition of NaOH does not result in a large amount of fume. The rate of fume generation from the melts containing NaOH under a N_2 purge was approximately equal to that with no NaOH present in the melt under a pure N_2 purge. During sulfide oxidation, the addition of NaOH suppressed the fume generation rate.

POTASSIUM AND CHLORIDE BEHAVIOR DURING FUME GENERATION

One of the major areas of concern with fume generation in the kraft recovery furnace is the behavior of Cl and K. Deposits in the upper stages of the furnace are enriched in these elements. The Cl and K lower the melting point of the deposits, which may result in harder and thicker deposits or a corrosive environment.

Reeve et al.[4] have reported a significant enrichment in the Cl and K content of the precipitator dust compared to the smelt. By comparing the molar ratio of Cl/Na in the precipitator dust to its ratio in the smelt, Reeve et al.[4] found an average enrichment of 1.4 for three West Coast Mills. For K, the comparison of the molar ratio of K/Na in the precipitator dust to the ratio in the smelt showed an average enrichment ratio of 2.0.

To determine what enrichment would be result from oxidative fuming, the K/Na molar ratios in fume generated from melts containing different K concentrations were compared to the K/Na ratio in the melt. Table 17, shows the fume generation rate and the K/Na ratio in the fume for melts containing different K levels.

The fume generation rate during sulfide oxidation in the K_2CO_3/Na_2CO_3 melts appears to be independent of the K/Na levels in the melt. The fume generation rate in a K_2CO_3/Na_2S melt is nearly the same as the fume generation rate in a Na_2CO_3/Na_2S melt. The K/Na ratios in the fume are approximately the same as the K/Na ratios in the melt; there is no enrichment of K in the fume.

Table 17. Effect of potassium on fume generation.

Conditions: Temp. = 955°C (1750°F)
O_2 Flow Rate = 0.021 L/min
N_2 Flow Rate = 1.0 L/min

| Initial Melt Composition | | | | | | |
Na_2CO_3, mole	K_2CO_3, mole	Na_2S mole	K/Na Molar Ratio	Fume Generation Rate (g/min) ± Std. Dev.	K/Na Molar Ratio	Enrichment Factor
0.76	0.01	0.03	0.0132	0.0766 ± 0.0034	—	
0.75	0.02	0.03	0.0256	0.0750 ± 0.0032	0.0225	0.88
0.73	0.04	0.03	0.0526	0.0765 ± 0.0024	—	
0.71	0.06	0.03	0.0811	0.0765 ± 0.0020	0.0888	1.09
0.69	0.08	0.03	0.111	0.0709 ± 0.0071	—	
0.67	0.10	0.03	0.143	0.0683 ± 0.0068	0.141	0.99
0.57	0.20	0.03	0.333	0.067 ± 0.0020	—	
0.37	0.40	0.03	1.00	0.058 ± 0.0030	0.96	0.96
0.10	0.71	0.03	5.46	0.053 ± 0.0060	6.01	1.10
0.0	0.77	0.03	25.7	0.073 ± 0.0050	—	

The behavior of Cl during oxidative fuming was studied by adding varying amounts of NaCl to Na_2CO_3-Na_2S melts. The Cl/Na ratios in the melts were chosen to be in the range of typical smelt samples as reported by Reeve et al.[4] Fume samples were collected from these melts under an inert atmosphere (N_2 purge only) and during sulfide oxidation (N_2-O_2 purge). These samples were analyzed for their Na and Cl content and the enrichment factor (the molar ratio of Cl/Na in the fume divided by the molar ratio of Cl/Na in the melt) was then calculated. The results of these experiments are shown in Table 18.

Table 18. Chloride enrichment during sulfide oxidation.

Conditions: Temp. = 955°C (1750°F)
             O_2 Flow Rate = 0.021 L/min
             N_2 Flow Rate = 1.0 L/min
             Melt Sulfidity = 20%

Melt Cl/Na Molar Ratio	Fume Cl/Na Molar Ratio	Enrichment Factor
0.10	0.86	8.4[a]
0.122	0.22	1.81
0.049	0.082	1.7

[a]N_2 purge only.

In the first experiment, Cl enrichment was measured with no O_2 in the purge. Based on its Cl content the fume obtained under this condition is 86% NaCl. This resulted in a Cl enrichment of 8.4 relative to the melt. Under oxidizing conditions, the Cl content in the fume was enriched by a factor of 1.7 to 1.8. This compares closely with the enrichment factor of 1.6 reported by Keitanniemi[23] and 2.0 reported by Reeve[4] for kraft mills.

With no chloride present in the melt, no K enrichment was observed in fume. To determine the effect of chloride on potassium enrichment, various levels of KCl and NaCl were added to the melt, and the fume generated under oxidizing conditions was analyzed for K and Cl. The results of these experiments are shown in Table 19.

The Cl and K levels used in these experiments were selected to be similar to those of typical kraft smelt. With Cl present in the melt, the enrichment factor for K ranged from 1.9 to 2.6. This range compares favorably with the enrichment factor of 1.8 to 2.0 reported by Reeve and 1.6 reported by Keitanniemi[23] for kraft mills.

Table 19. Effect of chloride on potassium enrichment during
           sulfide oxidation.

Conditions: Temp. = 955°C (1750°F)
             O_2 Flow Rate = 0.021 L/min
             N_2 Flow Rate = 1.0 L/min
             Melt Sulfidity = 20%

Melt		Fume		Enrichment Factor	
Cl/Na Molar	K/Na Ratio	Cl/Na Molar	K/Na Ratio	Cl	K
0.119	0.019	0.181	0.0492	1.5	2.62
0.127	0.028	0.169	0.0564	1.3	2.02
0.116	0.013	0.196	0.0272	1.7	2.11
0.123	0.061	0.183	0.115	1.5	1.89

These results indicate that the mechanism for K enrichment in the fume
is through the evolution of KCl. At the temperature of these experiments
(955°C), the vapor pressure of KCl (8.7 mm Hg) is approximately twice that of
NaCl (4.5 mm Hg). Therefore more KCl than NaCl evolves from the melt. Without
Cl in the melt, the fume would not be enriched in K.

Since the volatilities of NaCl and KCl are much greater than that of
Na_2CO_3, the fume produced under monoxidizing conditions consists almost entirely
of NaCl and KCl. The enhanced vaporization of Na_2CO_3 during sulfide oxidation
reduces the Cl enrichment factor to 2.0, which is similar to the enrichment
factor reported for kraft furnace.

If vaporization of NaCl and KCl is an equilibrium controlled process,
the vaporization rates of these compounds may be calculated, using Raoult's Law
Eq. (41) and assuming that the gas stream is saturated in these compounds.

$$P_{NaCl}(T) = P^*_{NaCl(T)} X_{NaCl} \qquad (41)$$

Here, $P_{NaCl(T)}$ is the equilibrium partial pressure of NaCl at temperature T;

$P^*_{NaCl(T)}$ is the vapor pressure of pure NaCl at temperature T; and

X_{NaCl} is the mole fraction of NaCl in the melt.

To determine if equilibrium processes controlled the vaporization of

NaCl and KCl, the observed vaporization rates were compared to the equilibrium

vaporization rates for the melts in Table 20.

Table 20. Melt compositions used in comparison of predicted and observed
           vaporization rates.

Purge Rate N_2 = 1.0 L/min, O_2 = 0.10 L/min

Run No	Temperature, °C	Melt Composition			
		Na_2CO_3, mole	NaCl, mole	KCl, mole	Na_2S, mole
344	954	0.565	0.16	0.03	0.14
345	954	0.565	0.16	0.45	0.14
346	954	0.546	0.16	0.02	0.14

The vaporization rates of these species can be calculated using their

vapor pressures and their mole fractions in the melt. For example, the rate of

vaporization of NaCl in Run 344 is shown below.

Vaporization rate = molar gas flow rate

x partial pressure of the volatile species

$$= \frac{1 \text{ L/min}}{22.4 \text{ L/mole}} \left| \frac{4.5 \text{ mmHg}}{760 \text{ mmHg}} \right| 0.208 = 5.5 \times 10^{-5} \frac{\text{mole}}{\text{min}}$$

The equilibrium predicted and actual vaporization rates of NaCl and KCl

for the three melts are shown in Table 21. The actual vaporization rates of

NaCl and KCl were calculated from the total fume generation rate and the NaCl

and KCl levels in the fume.

Table 21. Predicted and measured vaporization rates of NaCl and KCl.

Run	NaCl Vaporization		KCl Vaporization	
	Predicted, moles/min	Actual, moles/min	Predicted, moles/min	Actual, moles/min
344	5.5×10^{-5}	5.3×10^{-5}	2.0×10^{-6}	2.5×10^{-6}
345	5.3×10^{-5}	5.2×10^{-5}	3.2×10^{-6}	2.9×10^{-6}
346	5.3×10^{-5}	6.6×10^{-5}	1.4×10^{-6}	1.8×10^{-6}

As shown in this table, the predicted and actual fuming rates are surprisingly close considering the experimental errors involved in the measurement of the fuming rates. For example, the measured fuming rate has a standard deviation of approximately 10% of its average value and the K determination has a standard deviation of 7.5% in run 346 and 20.0% in run 345.

These calculations demonstrate that the vaporization of NaCl and KCl is controlled by equilibrium processes. The vaporization rates of these species are accurately predicted by assuming that partial pressures of these species are described by Raoult's Law and the level of these species in the gas phase is in equilibrium with the level in the melt.

CONCLUSIONS

The major conclusions reached in this report are summarized below:

1. Fume production is a dynamic process, dependent on mass transfer processes and chemical reactions. This implies that fume in a kraft recovery furnace is more than an equilibrium phenomenon, and that fume is a potentially manipulatable process.

2. Sodium vaporization can be significant during sulfide oxidation in a $Na_2CO_3-Na_2S$ melt and result in large quantities of Na_2CO_3 fume. This was an unexpected result, since Na is a reduced species and was previously not thought to be present during an oxidative process.

3. Fume produced during sulfide oxidation results from the oxidation of Na vapor in the gas phase. This oxidation of Na produces a Na sink in the gas phase, reducing the partial pressure of Na and the mass transfer resistance to vaporization. This vapor sink significantly increases the rate of Na vaporization.

4. Only when the purge was introduced below the melt's surface did sulfide oxidation produce sufficient quantities of fume. The oxidation of sulfide in a quiescent melt with the N_2-O_2 purge introduced above the melt's surface produced little fume. In this situation, the volatile species were oxidized before they could evolve from the melt. With the N_2-O_2 purge introduced below the melt's surface, the melt at the interface was renewed faster than it was oxidized. Volatile species were then present at the interface and produced large quantities of fume.

5. Fume generation resulting from reduction of Na_2CO_3 with
    carbon, H_2 or CO is significantly less than fume generation
    during sulfide oxidation in a well mixed melt. The addition
    of CO to the purge in a Na_2CO_3/Na_2S melt did not result in an
    increased level of fume generation over that observed with a
    N_2 purge. The addition of carbon in the form of kraft or
    soda char and the addition of H_2 to a Na_2CO_3/Na_2S melt
    only slightly increased the level of fume generation over
    that observed under a N_2 purge.

6. The addition of NaOH pellets to a Na_2CO_3/Na_2S melt did not
    result in any increase in fume generation. Sodium hydroxide
    levels as great as 4.5% did not result in significant fume.
    No evidence was obtained that the presence of NaOH in the
    melt contributes to fume.

7. Sodium and potassium chloride are more volatile than Na_2CO_3
    and K_2CO_3. This results in the fume being enriched in Cl.
    Since KCl is more volatile than NaCl, the fume is also enriched
    in K. Equilibrium considerations may govern the volatilization
    of NaCl and KCl.

8. The only volatile species that contribute to the formation of
    fume in the kraft furnace are Na vapor, K vapor, NaCl vapor
    and KCl vapor.

    a) No evidence was found for NaOH volatilizing as such
        from a carbonate melt and forming NaOH vapor.

    b) No evidence was found to support a role played by
        volatile alkali metal oxides.
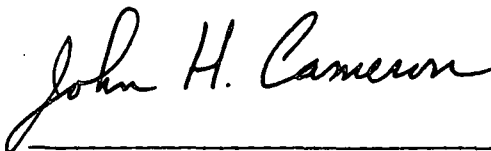
ACKNOWLEDGMENTS

LITERATURE CITED

1. Borg, A.; Teder, A.; Warnqvist, B., Tappi 57(1):126-9(Jan., 1974).

2. Warnqvist, B., Svensk Papperstid. 76(12):463-6(1973).

3. Spanbauer, J., Southern Pulp and Paper, Nov., 1982.

4. Reeve, D. W.; Hoc, N. T.; Barham, D., Tappi 64(5):109-13(May, 1981).

5. Rizhinshvili, G. V.; Kaplun, L. V., Bumazh. Prom. (1):26-8(Jan., 1983).

6. Turkdogan, E. T.; Grieveson, P.; Darken, L. S., J. Phys. Chem. 67:1647 (1963).

7. Turkdogan, E. T. Physical chemistry of high temperature technology. Academic Press, New York, 1980.

8. Turkdogan, E. T.; Grieveson, P.; Darken, L. S. Proc. Natl. Hearth Steel Con. 470(1982).

9. Merriam, R. L. Kraft, version 2.0, prepared for The American Paper Institute, New York, NY, Dec., 1980.

10. Cameron, J. H.; Grace, T. M., Ind. Eng. Chem. Fundam. 24(4):443(1985).

11. Cameron, J. H.; Grace, T. M. A kinetic study of carbon oxidation in an alkali carbonate melt, Project 3473-1, Progress Report Three, The Institute of Paper Chemistry, Appleton, WI, Feb., 1985.

12. Grace, T. M.; Cameron, J. H.; Clay, D. T. Char burning, Project 3473-6, The Institute of Paper Chemistry, Feb. 22, 1985.

13. Andresen, R. E., J. Electrochem. Soc., Feb., 1979:328-34.

14. Appleby, A. J.; Nicholson, S. J. Electroanal. Chem. 38, App. 13, 1977.

15. Brewer, L.; Mastick, D. F., J. Am. Chem. Soc. 73:2045(1951).

16. Motzfeld, K., J. Phys. Chem. 59:139(1955).

17. Bauer, T. W.; Dorland, R. M., Can. J. Techn. 32:91(1954).

18. Darken, L. S.; Turkdozan, E. T. Heterogeneous kinetics at elevated temperatures, edited by G. R. Belton and W. L. Worrell, Plenum Press, New York, 1970.

19. Leibson, I.; Holcomb, E. G.; Cacoso, A. G.; Jacmic, J. J., AIChE J., 296, (Sept., 1956).

20. Higbie, R., Trans. AIChE 31:365(1935).

21. Wilke, C. R.; Lee, C. Y., Ind. Eng. Chem. 47:1253(1955).

22. Hirschfelder, J. O.; Bird, R. B.; Spotz, E. L., Trans. Am. Soc. Mech. Engrs. 71:921(1949).

23. Keitaanniemi, O.; Virkola, N., Paperi Puu 60(9):507(1978).

THE INSTITUTE OF PAPER CHEMISTRY

John H. Cameron
Research Associate
Recovery Group
Chemical Sciences Division

Tom Grace
Group Leader, Recovery
Pulping Sciences
Chemical Sciences Division